

**Ferrocyanide Safety Project  
Task 3 Ferrocyanide Aging Studies  
FY 1994 Annual Report**

M. A. Lilga  
E. V. Alderson  
D. J. Kowalski  
M. R. Lumetta  
G. F. Schiefelbein

September 1994

Prepared for  
Westinghouse Hanford Company  
Waste Tank Safety Program  
with the U.S. Department of Energy  
under Contract DE-AC06-76RLO 1830

Pacific Northwest Laboratory  
Richland, Washington 99352

**MASTER**

**DISTRIBUTION OF THIS DOCUMENT IS UNLIMITED**

## **DISCLAIMER**

**This report was prepared as an account of work sponsored by an agency of the United States Government. Neither the United States Government nor any agency thereof, nor any of their employees, make any warranty, express or implied, or assumes any legal liability or responsibility for the accuracy, completeness, or usefulness of any information, apparatus, product, or process disclosed, or represents that its use would not infringe privately owned rights. Reference herein to any specific commercial product, process, or service by trade name, trademark, manufacturer, or otherwise does not necessarily constitute or imply its endorsement, recommendation, or favoring by the United States Government or any agency thereof. The views and opinions of authors expressed herein do not necessarily state or reflect those of the United States Government or any agency thereof.**

## **DISCLAIMER**

**Portions of this document may be illegible in electronic image products. Images are produced from the best available original document.**

## Summary

This annual report gives the results of the work conducted by the Pacific Northwest Laboratory in FY 1994 on Task 3 of the Ferrocyanide Safety Project, Ferrocyanide Aging Studies. Waste aging refers to the dissolution and hydrolysis of simulated Hanford ferrocyanide waste in alkaline aqueous solutions by radiolytic and chemical means. The ferrocyanide simulant primarily used in these studies was In-Farm-1B, Rev. 7, prepared by Westinghouse Hanford Company to simulate the waste generated when the In-Farm flowsheet was used to remove radiocesium from waste supernates in single-shell tanks at the Hanford Site. In the In-Farm flowsheet, nickel ion and ferrocyanide anion were added to waste supernate to precipitate sodium nickel ferrocyanide and co-precipitate radiocesium. Once the radiocesium was removed, supernates were pumped from the tanks, and new wastes from cladding removal processes or from evaporators were added. These new wastes were typically highly caustic, having hydroxide ion concentrations of over 1 M and as high as 4 M. Reactions that this caustic waste may have had with the precipitated ferrocyanide waste in a radiation field are the subject of the Aging Studies task.

In previous Aging Studies research,  $\text{Na}_2\text{NiFe}(\text{CN})_6$  in simulants was shown to dissolve in basic solutions, forming insoluble  $\text{Ni}(\text{OH})_2$  and soluble  $\text{Na}_4\text{Fe}(\text{CN})_6$ . The influence on solubility of base strength, sodium ion concentration, anions, and temperature was previously investigated. Destruction of ferrocyanide anion by hydrolysis to form ammonia and formate ion was found to be promoted by gamma radiolysis.

In FY 1994 research, the hydrolysis reaction was studied in more detail. Ammonia production as a function of time was determined in experiments containing 2 M NaOH in which temperature (50°C, 70°C, and 90°C), gamma radiation dose rate ( $1.07 \times 10^5$ ,  $4.25 \times 10^4$ , and  $8.91 \times 10^3$  Rad/h), and ferrocyanide anion concentration (0.0063, 0.0127, and 0.0254 M) were varied. Ammonia yields after 12 days were found to be an order of magnitude higher in the gamma-irradiated samples compared with identical, but not irradiated, controls. Ammonia yields also increased with increasing temperature, gamma radiation dose, and ferrocyanide concentration. However, at a dose rate of  $1.07 \times 10^5$  Rad/h, the extent of hydrolysis at 70°C and 50°C was only about 3% and 0.2%, respectively, compared with about 90% at 90°C, based on moles cyanide, primarily in the form of soluble ferrocyanide ion, and the observed ammonia concentration. Hydrolysis in other experiments ranged from 20% to 70%. Yields are approximate since ammonia itself was found to be destroyed in the gamma environment. A zero-order rate constant of  $1.3 \times 10^{-3}$  moles/L/day at a dose rate of  $1.07 \times 10^5$  Rad/h was measured for this process.

Ammonia production as a function of time was sigmoidal, with an induction period of about 7 days, during which time ammonia was produced slowly, followed by a period of relatively rapid ammonia generation, in turn followed by a leveling-off and often decreasing solution ammonia concentration. The concentration of soluble iron species usually remained constant at about the starting concentration for several days before dropping off in what appeared to be a pseudo-first-order manner. The long induction period and the behavior of soluble iron seemed indicative of the formation of one or

more intermediates prior to destruction of the majority of the cyanide ions. The identity of these intermediates is unknown at this time, but likely involves ligand-substituted iron cyanides and may involve binuclear or higher iron cluster complexes. The leveling-off and decrease in ammonia concentration was not necessarily indicative of complete ferrocyanide destruction but, rather, resulted when the rate of ammonia destruction in the gamma field exceeded the rate of production by hydrolysis.

The change in concentration of formate ion, also a product of cyanide hydrolysis, generally paralleled that of ammonia. The hydrolysis reaction should form one equivalent of ammonia and one equivalent of formate. However, the formate ion concentration was up to five times less than that of ammonia and decreased rapidly when hydrolysis slowed. The results suggest that formate ion is destroyed by gamma radiation more efficiently than is ammonia.

The concentration of soluble nickel tended to increase during the hydrolysis experiments, as well as in a control experiment in which the  $[\text{CN}^-]$  was varied in solutions allowed to equilibrate with solid  $\text{Ni}(\text{OH})_2$ . Free cyanide ion liberated during ferrocyanide destruction resolubilized the nickel, presumably as a nickel cyanide complex.

Hydrolysis occurred slowly at pH 10, presumably because  $\text{Na}_2\text{NiFe}(\text{CN})_6$  has very low solubility in this medium. An ammonia yield of at least 4% was obtained after 3 months of irradiation and heating to 60°C. Gamma radiation promoted hydrolysis at this pH; an order of magnitude more hydrolysis occurred in the gamma field than in controls that were not irradiated.

Aluminum in the hydrolysis solution had relatively little effect. However, it may have slightly promoted hydrolysis.

Also investigated was the competition of ferrocyanide simulant dissolution with the ion exchange of cesium, which forms an insoluble cesium-containing nickel ferrocyanide. A ferrocyanide simulant (unwashed "Vendor" material), which does not contain cesium, was stirred with aqueous base containing cesium at room temperature. Cesium uptake was found to be more rapid than dissolution. The cesium concentration was decreased to the detection limit (98% removal) within 2 min, the time the first solution sample was taken. The ferrocyanide dissolution was about 70% to 80% complete in the same time period, depending on the starting cesium concentration. In addition, the ferrocyanide dissolution was incomplete, reaching 85% after 24 h of stirring for the solution containing the highest starting cesium concentration. Incomplete dissolution is consistent with the previous observation that cesium-containing nickel ferrocyanides have very low solubility in aqueous base.

# Contents

Summary .....	iii
Abbreviations .....	xi
1.0 Introduction .....	1.1
2.0 Work Accomplished .....	2.1
2.1 Experimental .....	2.1
2.1.1 Materials and Methodology .....	2.1
2.1.2 Description of the Gamma Facility, Gamma Dose Rate Cross Sections for Irradiated Solutions, and Estimation of Integrated Dose .....	2.3
2.1.3 Analytical Methods .....	2.7
2.2 Cesium Ion Exchange in Competition with Ferrocyanide Dissolution .....	2.10
2.3 Hydrolysis of In-Farm Ferrocyanide Flowsheet Material in 2 M NaOH .....	2.13
2.3.1 Dependence of Hydrolysis on Temperature .....	2.14
2.3.2 Dependence of Hydrolysis on Gamma Dose Rate .....	2.22
2.3.3 Dependence of Hydrolysis on Ferrocyanide Ion Concentration .....	2.28
2.4 Hydrolysis of In-Farm Ferrocyanide Flowsheet Material at pH 10 .....	2.31
2.5 Hydrolysis of In-Farm Ferrocyanide Flowsheet Material in the Presence of an Aluminum Decladding Waste Simulant .....	2.34
3.0 Conclusions .....	3.1
4.0 References .....	4.1

## Figures

2.1	Gamma Dose Rate Cross Sections for Tubes Used in Hydrolysis Experiments Conducted at an Average of $1.07 \times 10^5$ Rad/h . . . . .	2.4
2.2	Gamma Dose Rate Cross Sections for Tubes Used in Hydrolysis Experiments Conducted at an Average of $4.25 \times 10^4$ Rad/h . . . . .	2.5
2.3	Gamma Dose Rate Cross Sections for Tubes Used in Hydrolysis Experiments Conducted at an Average of $8.91 \times 10^3$ Rad/h . . . . .	2.6
2.4	Measured Versus Generated Ammonia Concentration in Experiments Not Gamma Irradiated . . . . .	2.9
2.5	Ammonia Concentration as a Function of Time Irradiated at a Gamma Dose Rate of $1.07 \times 10^5$ Rad/h . . . . .	2.10
2.6	Dissolution and Cesium Ion Exchange in 3 and 4 M NaOH at an Initial [Cs] of $2.3 \times 10^{-3}$ M . . . . .	2.11
2.7	Dissolution and Cesium Ion Exchange in 4 M NaOH at $2.3 \times 10^{-3}$ M and $3 \times 10^{-4}$ M Initial Cesium Ion Concentration . . . . .	2.12
2.8	Dissolution Behavior of a Solid In-Farm Flowsheet Material Containing Cesium Ion Compared with a Solid Vendor-prepared Simulant Not Containing Cesium . . . . .	2.13
2.9	Ammonia and Formate Ion Production in the Hydrolysis of IF-1B in 2 M NaOH at $90^\circ\text{C}$ and $1.07 \times 10^5$ Rad/h (H1) . . . . .	2.15
2.10	Temperature Dependence of Ammonia Production in the Hydrolysis of IF-1B (0.5 g) at a Gamma Dose Rate of $1.07 \times 10^5$ Rad/h (H1) . . . . .	2.17
2.11	Temperature Dependence of Ammonia Production in the Hydrolysis of IF-1B (0.5 g) at a Gamma Dose Rate of $1.07 \times 10^5$ Rad/h (H1), Expanded View . . . . .	2.17
2.12	Total Iron Concentration in the Hydrolysis of IF-1B (0.5 g) at $90^\circ\text{C}$ and at a Gamma Dose Rate of $1.07 \times 10^5$ Rad/h (H1) . . . . .	2.18
2.13	First-order Plot for the Change in Iron Concentration in the Hydrolysis of IF-1B (0.5 g) at $90^\circ\text{C}$ and at a Gamma Dose Rate of $1.07 \times 10^5$ Rad/h (H1) . . . . .	2.18

2.14	Changes in Nitrate and Nitrite Ion Concentrations and the Sum of These Concentrations in the Hydrolysis of IF-1B (0.5 g) at 90°C and at a Gamma Dose Rate of $1.07 \times 10^5$ Rad/h (H1) . . . . .	2.19
2.15	Temperature Dependence of Nitrate Destruction in the Hydrolysis of IF-1B (0.5 g) at a Gamma Dose Rate of $1.07 \times 10^5$ Rad/h . . . . .	2.20
2.16	Temperature Dependence of Nitrite Formation in the Hydrolysis of IF-1B (0.5 g) at a Gamma Dose Rate of $1.07 \times 10^5$ Rad/h . . . . .	2.20
2.17	Total Nickel Concentration in the Hydrolysis of IF-1B (0.5 g) at 90°C and at a Gamma Dose Rate of $1.07 \times 10^5$ Rad/h (H1) . . . . .	2.21
2.18	Equilibrium Free Cyanide Ion Versus Nickel Concentrations for the Nickel Redissolution Control Experiments Determined by Ion Selective Electrode . . . . .	2.23
2.19	Plot of $[\text{CN}^-]^2$ Versus $[\text{Ni}]$ for Nickel Redissolution Control Experiments at Equilibrium . . . . .	2.23
2.20	Gamma Dose Rate Dependence of Ammonia Production as a Function of Time in the Hydrolysis of IF-1B (0.5 g) at 90°C . . . . .	2.25
2.21	Ammonia Production as a Function of Integrated Dose ( $\text{Rad} \times 10^{-7}$ ) . . . . .	2.25
2.22	Formate Ion Production in the Hydrolysis of IF-1B in 2 M NaOH at 90°C and at Gamma Dose Rates of $4.25 \times 10^4$ Rad/h (H4) and $8.91 \times 10^3$ Rad/h (H5) . . . . .	2.26
2.23	Total Iron Concentration as a Function of Time in the Hydrolysis of IF-1B (0.5 g) at 90°C and at Gamma Dose Rates of $4.25 \times 10^4$ Rad/h (H4) and $8.91 \times 10^3$ Rad/h (H5) . . . . .	2.26
2.24	Gamma Dose Rate Dependence of Nitrate Destruction in the Hydrolysis of IF-1B (0.5 g) at 90°C . . . . .	2.27
2.25	Gamma Dose Rate Dependence of Nitrite Formation in the Hydrolysis of IF-1B (0.5 g) at 90°C . . . . .	2.28
2.26	Rate Constants for Nitrate Ion Destruction as a Function of Gamma Dose Rate . . . . .	2.29
2.27	Dependence of Ammonia Production on Initial Ferrocyanide Ion Concentration in Hydrolysis of IF-1B at 90°C and at a Gamma Dose Rate of $1.07 \times 10^5$ Rad/h . . . . .	2.30
2.28	Dependence of Formate Ion Production on Initial Ferrocyanide Ion Concentration in Hydrolysis of IF-1B at 90°C and at a Gamma Dose Rate of $1.07 \times 10^5$ Rad/h . . . . .	2.31

2.29	Total Iron Concentration as a Function of Time in Hydrolysis of IF-1B [0.0254 M $\text{Fe}(\text{CN})_6^{4-}$ ] at 90°C and at a Gamma Dose Rate of $1.07 \times 10^5$ Rad/h (H7) . . . . .	2.32
2.30	Ferrocyanide Ion Concentration Dependence of Nitrate Destruction in the Hydrolysis of IF-1B at 90°C and at a Gamma Dose Rate of $1.07 \times 10^5$ Rad/h . . . . .	2.32
2.31	Ferrocyanide Ion Concentration Dependence of Nitrite Formation in the Hydrolysis of IF-1B at 90°C and at a Gamma Dose Rate of $1.07 \times 10^5$ Rad/h . . . . .	2.33
2.32	Ammonia Production in Hydrolysis of IF-1B (0.5 g) at 90°C and at a Gamma Dose Rate of $1.07 \times 10^5$ Rad/h in the Absence (H1) and in the Presence (H9) of Aluminum . . . . .	2.35
2.33	Measured Versus Known Ammonia Concentrations in Standard Solutions Containing Aluminum . . . . .	2.36
2.34	Formate Ion Production in Hydrolysis of IF-1B (0.5 g) at 90°C and at a Gamma Dose Rate of $1.07 \times 10^5$ Rad/h in the Absence (H1) and in the Presence (H9) of Aluminum . . . . .	2.36
2.35	Total Iron Concentration as a Function of Time in Hydrolysis of IF-1B (0.5 g) at 90°C and at a Gamma Dose Rate of $1.07 \times 10^5$ Rad/h in the Presence of Aluminum (H9) . . . . .	2.37

## Tables

2.1	Analysis of IF-1B Dissolved in 2 M NaOH or en/EDTA . . . . .	2.2
2.2	Estimation of Integrated Gamma Dose in Hydrolysis Experiments at Various Dose Rates for the First and Last Samples Taken . . . . .	2.7
2.3	Ferrocyanide Hydrolysis Variables Investigated . . . . .	2.14
2.4	Conditions for IF-1B Hydrolysis Experiments Investigating the Effect of Temperature Variation. . . . .	2.14
2.5	Rate Constants for Nitrate Destruction and Nitrite Formation at Various Temperatures . . .	2.21
2.6	Conditions for IF-1B Hydrolysis Experiments Investigating the Effect of Gamma Dose Rate Variation. . . . .	2.24
2.7	Rate Constants for Nitrate Destruction and Nitrite Formation at Various Gamma Dose Rates . . . . .	2.28
2.8	Conditions for IF-1B Hydrolysis Experiments Investigating the Effect of Ferrocyanide Ion Concentration Variation. . . . .	2.29
2.9	Rate Constants for Nitrate Destruction and Nitrite Formation at Various Gamma Dose Rates . . . . .	2.33
2.10	Neutralized Aluminum Coating Waste Composition Estimated from the Bismuth Phosphate Process and Composition of the Simulant Used for Hydrolysis Experiment H9 . . . . .	2.34



## Abbreviations

AA	atomic absorption spectroscopy
DOE	U.S. Department of Energy
EDTA	ethylenediaminetetraacetic acid
EIS	Environmental Impact Statement
en	ethylenediamine
FECN-14	PNL-prepared cesium nickel ferrocyanide material
GAO	General Accounting Office
IC	ion chromatography
IF-1A	In-Farm-1A, Rev. 4, WHC-prepared flowsheet ferrocyanide material
IF-1B	In-Farm-1B, Rev. 7, WHC-prepared flowsheet ferrocyanide material
ISE	ion selective electrode
PNL	Pacific Northwest Laboratory
SST	single-shell storage tank at Hanford
TBP	tributyl phosphate
USQ	unreviewed safety question
"Vendor" material	unwashed ferrocyanide simulant containing $\text{Na}_2\text{NiFe}(\text{CN})_6$ , $\text{Na}_2\text{SO}_4$ , and $4.5 \text{ H}_2\text{O}$ , as determined by chemical analysis, prepared by an outside vendor
WHC	Westinghouse Hanford Company

## 1.0 Introduction

The research performed for this project is part of an effort begun in the mid-1980s to characterize the materials stored in the single-shell waste storage tanks (SSTs) at the U.S. Department of Energy (DOE) Hanford Site. Various radioactive wastes from defense operations have accumulated at the Hanford Site in underground waste tanks since the early 1940s. During the 1950s, additional tank storage space was required to support the defense mission. Hanford Site scientists developed two procedures to obtain this additional storage volume within a short time period without constructing more storage tanks. One procedure involved the use of evaporators to concentrate the waste by removing water. Another procedure involved developing precipitation processes for scavenging radiocesium and other soluble radionuclides from tank waste liquids.

In radiocesium scavenging processes, waste solutions were adjusted to a pH between 8 and 10; and sodium or potassium ferrocyanide and nickel sulfate were added to co-precipitate cesium with the insoluble alkali-metal nickel ferrocyanide. Because waste solutions had high nitrate and radiolytically produced nitrite concentrations, these ions became incorporated into the precipitates. After the radioactive precipitates settled, the decontaminated solutions were pumped to disposal cribs, thereby providing the additional tank storage volume. Much later, some of the tanks were "stabilized" against leakage by removing pumpable liquids from the tanks, leaving behind a wet solid (sludge) residue containing the ferrocyanide precipitates (Burger et al. 1991). In implementing this process, approximately 140 metric tons of ferrocyanide [calculated as  $\text{Fe}(\text{CN})_6^{-4}$ ] were added to waste that was later routed to 20 large (500,000- to 750,000-million-gal) underground SSTs. Records at Hanford show 18 SSTs contain at least 200 kg (1000 g-mol) of ferrocyanide precipitates. The ferrocyanide content of the individual tanks ranges from 200 kg up to possibly 16,600 kg in Tank BY-104 (Borsheim and Simpson 1991).

Three flowsheets were used to scavenge the radiocesium from aqueous wastes. The T-Plant flowsheet, used to treat first-cycle waste from the bismuth phosphate process, generated about 8% of the total ferrocyanide waste. The U-Plant flowsheet treated "metal waste" dissolved in nitric acid after the uranium had been recovered using the tributyl phosphate (TBP) process. The U-Plant flowsheet produced about 66% of the total ferrocyanide waste. The third process, the In-Farm flowsheet, treated the basic waste from recovery of uranium. This process produced the remaining 26% of the total ferrocyanide waste.

Unlike the In-Farm flowsheet waste, T-Plant and U-Plant flowsheet waste contained substantial metal concentrations that precipitated when neutralized with sodium hydroxide. The ferrocyanide was thereby diluted, assuming that the solids-settling behaviors of the metal species and ferrocyanides were approximately the same. Although the In-Farm flowsheet produced only about a quarter of the ferrocyanide waste, the concentration of ferrocyanide in the waste is anticipated to be significantly higher than that in the T-Plant and U-Plant waste. Prepared In-Farm and U-Plant flowsheet simulants, which are representative of these wastes, contain about 25 wt% and 8 wt% ferrocyanide ion (dried simulants), respectively.

As part of waste management operations, after the ferrocyanide waste was precipitated and the supernate removed, aluminum decladding waste and/or evaporator bottoms from the concentration of reprocessing wastes were added to the tanks (Anderson 1990). These solutions were generally quite alkaline, containing NaOH concentrations of 1 to 2 M, with occasional additions of up to 4 M NaOH.

Concern has been raised about the safety of ferrocyanide waste intermixed with oxidants, such as nitrate and nitrite salts. In the laboratory, such mixtures can be made to undergo uncontrolled or explosive reactions by heating dry reagents to over 200°C. For example, mixtures of cesium zinc ferrocyanide and nitrate explode when heated (Hepworth et al. 1957). The 1987 Environmental Impact Statement (EIS), *Final Environmental Impact Statement, Disposal of Hanford Defense High-Level Transuranic and Tank Waste, Hanford Site, Richland, Washington* (DOE 1987), included an environmental impact analysis of potential explosions involving ferrocyanide-nitrate mixtures. The EIS postulated that an explosion could occur during mechanical retrieval of saltcake or sludge from a ferrocyanide waste tank. The EIS concluded that this worst-case accident could create enough energy to release radioactive material to the atmosphere through ventilation openings, exposing persons offsite to a short-term radiation dose of approximately 200 mrem. A General Accounting Office (GAO) study (Peach 1990) postulated a greater worst-case accident, with independently calculated doses of one to two orders of magnitude greater than that postulated in the DOE EIS. Uncertainties regarding the safety envelope of the Hanford Site ferrocyanide waste tanks led to the declaration of the ferrocyanide unreviewed safety question (USQ) in October 1990 (Deaton 1990). A special Hanford Ferrocyanide Task Team was commissioned to address all technical aspects involving SSTs containing ferrocyanide wastes. The Hanford Ferrocyanide Task Team is composed of technical experts from Westinghouse Hanford Company (WHC), Pacific Northwest Laboratory (PNL)<sup>(a)</sup>, and outside consultants.

Numerous studies conducted by the Task Team resulted in closure of the USQ in March 1994. The potential for ferrocyanide reactions in Hanford Site SSTs was evaluated and the energy released during these reactions was quantified (Burger 1984; Burger and Scheele 1988, 1991; Cady 1993; Hallen et al. 1992; Scheele and Cady 1992; Scheele et al. 1991, 1992). Recently, dynamic X-ray diffraction has been used to identify specific reactions and to quantify reaction rates (Dodds and Thompson 1994). In addition, a number of experimental and theoretical studies have been conducted in an effort to analyze the thermal characteristics of the tanks (Crowe et al. 1993; McLaren 1993, 1994; McLaren and Cash 1993) and to investigate the likelihood of "hot spots" forming as a result of radiolytic heating (Epstein and Fauske 1994; McGrail et al. 1993). The measured temperatures in these tanks continue to drop, and the highest temperature currently recorded is 53°C (Meacham et al. 1994).

Safety criteria for ferrocyanide waste are based on the results of these thermal reactivity, tank characterization, and theoretical studies (Postma et al. 1994). The most important criteria are the concentration of ferrocyanide in the waste, the amount of free (unbound) water present, and the temperature of the waste. Waste is considered safe if it contains less than 8 wt%  $\text{Na}_2\text{NiFe}(\text{CN})_6$  (measured in dried waste with no free water), regardless of temperature, water content, or oxidant

---

(a) Operated for the U.S. Department of Energy by Battelle Memorial Institute under Contract DE-AC06-76RLO 1830.

content. Ferrocyanide waste is said to be conditionally safe if it contains more than 8 wt%  $\text{Na}_2\text{NiFe}(\text{CN})_6$ , contains up to 24 wt% free water, and is at a temperature less than  $90^\circ\text{C}$ . Tanks are categorized as unsafe if they contain higher ferrocyanide concentrations without adequate free water or contain waste at a temperature higher than  $90^\circ\text{C}$ . Two ferrocyanide-containing tanks are considered safe and the rest are classified conditionally safe. None fall in the category of unsafe. To resolve the ferrocyanide safety issue, tank contents must meet the safety criteria and operations must be conducted such that waste conditions fall within the criteria limits.

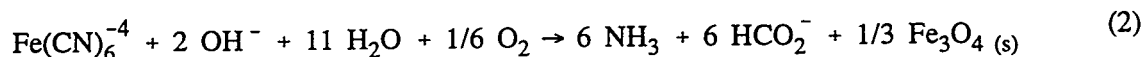
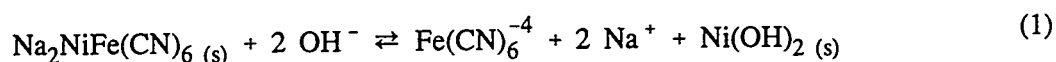
Because the ferrocyanide sludge has been exposed for many years to other highly caustic wastes, as well as to elevated temperatures and both gamma and beta radiation, ferrocyanide decomposition may have occurred in the tanks. As a result, the concentration of ferrocyanide may be much less than that predicted by tank inventory records. If so, tanks may then be re-categorized as safe, facilitating remediation.

The goal of the Aging Studies task is to understand the long-term chemical and radiolytic behavior of ferrocyanide tank wastes in the SST environments. In turn, this information provides baseline data that will be useful as actual SST samples are obtained and analyzed. The results of aging studies will directly assist in determining which strategy will assure safe storage of the ferrocyanide waste in the tanks and how the ferrocyanide safety issue can be resolved. In previous ferrocyanide waste aging studies utilizing flowsheet simulants (Lilga et al. 1992, 1993), redissolution of  $\text{Na}_2\text{NiFe}(\text{CN})_6$  in caustic solutions was shown to occur and was studied under a variety of conditions. Products of the dissolution are soluble  $\text{Fe}(\text{CN})_6^{4-}$  and insoluble  $\text{Ni}(\text{OH})_2$ . Destruction of  $\text{Fe}(\text{CN})_6^{4-}$  by hydrolysis was also demonstrated.

This report describes the results of FY 1994 research for the Aging Studies task, which focused on the hydrolysis of ferrocyanide waste simulants in aqueous base. Hydrolysis was investigated in 2 M NaOH as a function of temperature, applied gamma dose rate, and soluble  $\text{Fe}(\text{CN})_6^{4-}$  concentration. A hydrolysis experiment was conducted at pH 10 and another in the presence of aluminum. In addition, experiments investigating cesium ion exchange in competition with sodium nickel ferrocyanide dissolution were conducted.

## 2.0 Work Accomplished

Work conducted over the last 3 years on the Aging Studies task has addressed issues regarding how ferrocyanides in tank waste may have changed over decades of storage and after additions of other highly caustic wastes. Aging, as used here, is any process that may have altered the chemical nature of the ferrocyanide waste. In these studies, the primary aging routes that have been investigated are dissolution of alkali metal nickel ferrocyanides, shown in Eq. (1) for the sodium compound, and hydrolysis of ferrocyanide ion, shown in Eq. (2) for one reported stoichiometry (Robuck and Luthy 1989). Solubility investigations in FY 1994 were limited to studies of dissolution of sodium nickel ferrocyanide in competition with uptake of cesium from solution by ion exchange to form an insoluble cesium nickel ferrocyanide phase. Many other aspects of alkali metal nickel ferrocyanide solubility, including the insolubility of the cesium-containing materials, have been described in previous reports (Lilga et al. 1992, 1993).



Research conducted in FY 1994 has primarily been directed toward the destruction of ferrocyanide anion by hydrolysis in caustic solution under conditions approximating those in SSTs. The influence of gamma dose rate, temperature, and ferrocyanide ion concentration on hydrolysis in 2 M NaOH was examined. Experiments at pH 10 and in the presence of an aluminum coating waste simulant were also conducted. In addition, competition experiments investigating the rate of cesium ion exchange relative to the rate of dissolution of In-Farm flowsheet simulant were performed.

## 2.1 Experimental

This section describes the In-Farm flowsheet materials used and the experimental methodology. It also includes a discussion of the gamma facility, the gamma dose rate cross section experienced by irradiated solutions, and the analytical methods used.

### 2.1.1 Materials and Methodology

The ferrocyanide-containing material used in the hydrolysis studies was the In-Farm-1B, Rev 7 (IF-1B) flowsheet material prepared by WHC (Jeppson and Wong 1993). The wet sludge was dried to constant weight in a vacuum oven at 60°C and stored in a desiccator. The wet IF-1B material was found to contain 47.2 wt% water when dried under these conditions. Samples of the dried IF-1B were stirred in 2 M NaOH or aqueous 5% ethylenediamine (en)/5% ethylenediaminetetraacetic acid (EDTA),

and the supernate analyzed. Table 2.1 summarizes analytical results for iron (corresponding to soluble ferrocyanide), cesium, and nickel. The en/EDTA solvent dissolved all of the IF-1B starting material, while the NaOH solution did not. As previously discussed, aqueous NaOH does not dissolve " $\text{Cs}_2\text{NiFe}(\text{CN})_6$ " or other phases containing cesium (Bryan et al. 1993; Lilga et al. 1993).

**Table 2.1.** Analysis of IF-1B Dissolved in 2 M NaOH or en/EDTA

<u>Dissolving Medium</u>	<u>moles Fe/g IF-1B</u>	<u>moles Cs/g IF-1B</u>	<u>moles Ni/g IF-1B</u>
2 M NaOH	$6.35 \times 10^{-4}$	$< 7.31 \times 10^{-7}$	$1.49 \times 10^{-5}$
en/EDTA	$9.56 \times 10^{-4}$	$3.69 \times 10^{-5}$	$1.10 \times 10^{-3}$

Appropriately, the iron, cesium, and nickel concentrations in the NaOH solution were found to be lower than in the en/EDTA solution. The 2 M NaOH solution concentrations in Table 2.1 are representative of species concentrations in the starting solutions of most of the hydrolysis experiments, with the exception of those conducted at pH 10, in which sodium nickel ferrocyanide has low solubility.

Because experiments were conducted in the gamma facility, sequential sampling of one reaction solution to monitor changes in reactant and product concentrations was impractical. Instead, eight stainless steel vessels were charged with identical amounts and concentrations of reagents. Six vessels were lowered into tubes in the gamma pit for irradiation and two were left outside of the pit as controls. Placement of the vessels in the gamma pit tubes was adjusted to give gamma dose rates as consistent as possible for each of the six vessels (see Section 2.1.2). Temperature controllers were used in conjunction with heating tape wrapped around each vessel to maintain a stable, consistent temperature. Vessels were charged with IF-1B and argon-purged caustic solution, sealed, pressurized and vented two times with argon (to remove air), then pressure-checked with argon and vented to atmospheric pressure. Appropriate vessels were then introduced into the gamma pit and heating of all vessels begun. Heatup to 90°C took about 2 h. Temperatures and pressures were monitored and recorded with use of a Campbell Scientific 21X datalogger with battery backup utilizing an AM416 multiplexer, 107 Temperature probe, and Toshiba 3000 portable computer. Reaction solutions were unstirred.

In a typical experiment, reaction vessels were individually removed from the gamma pit after 2, 5, 7, 12, 16, and 19 days (Sample 1 to Sample 6, respectively). Controls were terminated after 12 and 19 days of reaction. Vessels were cooled to room temperature (cooling period 3 to 6 h), and a gas sample taken with a 75-mL evacuated sample vessel for mass spectral analysis. The 11-m-long (36-ft) stainless steel tubing connecting the reaction vessel to the monitoring/sampling panel was removed at the reaction vessel and replaced with a short connection to a GasTech  $\text{NH}_3$  sensing tube (colorimetric  $\text{NH}_3$  determination) and sampling pump. Typically, the pump plunger was withdrawn to the 50-mL calibration, and the  $\text{NH}_3$  concentration read directly from the tube. Because the gas-phase ammonia was an

insignificant fraction of the total ammonia produced (Section 2.1.3), the readings from the sensing tubes were used as qualitative indicators only. The reaction vessel was then sealed and returned to the laboratory for further analysis (Section 2.1.3).

The supernate was sampled (5 mL, unfiltered) and analyzed for solution  $\text{NH}_3$ . Another 5 mL were filtered through a 0.45- $\mu\text{m}$  Gelman Acrodisc syringe filter for atomic absorption (AA) and ion chromatography (IC) analyses. The remaining supernate was filtered through a 0.47- $\mu\text{m}$  magna nylon millipore filter, and the precipitate washed with de-ionized water. Precipitates were dried at 100°C.

### 2.1.2 Description of the Gamma Facility, Gamma Dose Rate Cross Sections for Irradiated Solutions, and Estimation of Integrated Dose

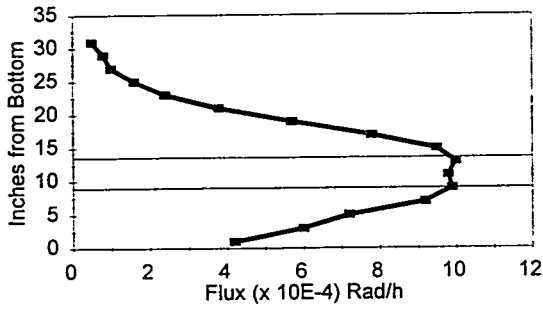
The Gamma Irradiation Facility operated by PNL contains 37 stainless steel irradiation tubes positioned in a 2.13-m-diameter (7-ft) by 4.17-m-deep (13-ft, 8-in.) stainless steel tank. Two arrays of  $^{60}\text{Co}$  with a combined inventory of 32 kCi are located near the bottom of the tank. For radiation shielding purposes, the tank is completely filled with water. A concrete wall, 1.07 m (3.5 ft) in height, surrounds the top of the tank. The irradiation tubes, which are sealed on the bottom, vary in length from 4.88 to 5.49 m (16 to 18 ft) and in diameter from 45.7 to 152.4 mm (1.8 to 6 in.). The irradiation flux of the tubes ranges from  $2 \times 10^6$  to  $2 \times 10^2$  Rad/h. The uniform flux region varies from about 152.4 mm (6 in.) for the tubes closest to the sources to greater than 304.8 mm (12 in.) for the tubes farthest away from the sources. All flux measurements in the tubes are traceable to the National Institute of Standards and Technology.

Materials, capsules, and test systems are lowered into the irradiation tubes, manually or by using a half-ton crane, to a depth giving the desired flux. They are left in the tubes for the required time, and, because there is no activation associated with the gamma irradiation, materials are transported to other facilities for examination after removal from the tubes.

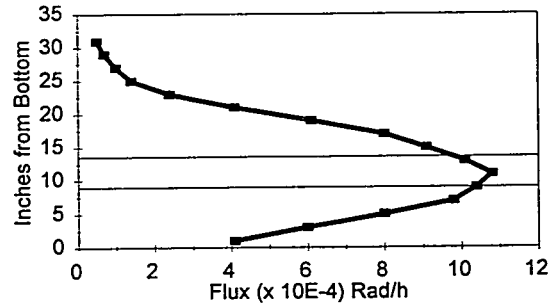
Figures 2.1 through 2.3 illustrate how the flux changes with depth in the tubes used in the hydrolysis experiments. The flux data shown are for February 1994. Over the course of the fiscal year (ending September 30, 1994), the flux in each tube decreased by about 7% because of the natural decay of the  $^{60}\text{Co}$  sources. Also shown on each graph is the position (top and bottom) of the reaction solutions within the tubes and the associated flux experienced by the solutions. Two different types of reaction vessels with different internal diameters were used in each experiment, resulting in different solution heights. The solution height for Vessels 1 through 3 (Sample 1 through Sample 3) was 117 mm; these vessels were used in tubes having a flat flux profile. Vessels 4 through 6 (Sample 4 through Sample 6), having a solution height of 35 mm, were used to minimize the flux variation within solutions in tubes where the flux had a larger variation with depth.

Integrated doses for samples irradiated at a flux of  $1.07 \times 10^5$ ,  $4.25 \times 10^4$ , or  $8.91 \times 10^3$  Rad/h are estimated in Table 2.2. The integrated dose received in the gamma pit experiments is comparable to

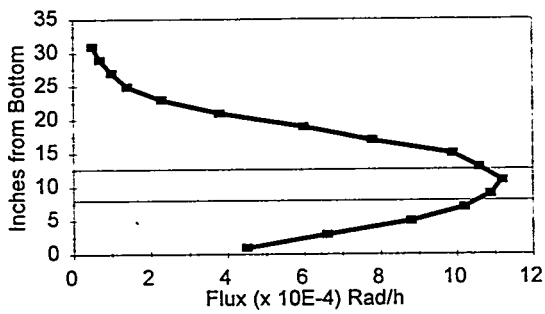
**Tube 18 (Sample 1)**



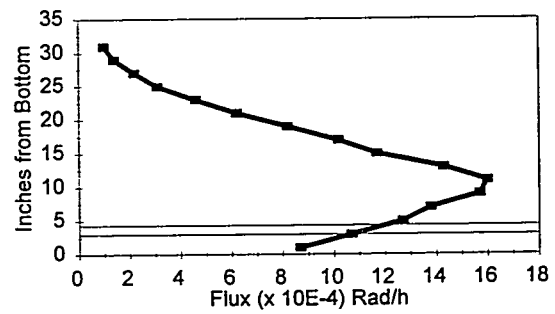
**Tube 19 (Sample 2)**



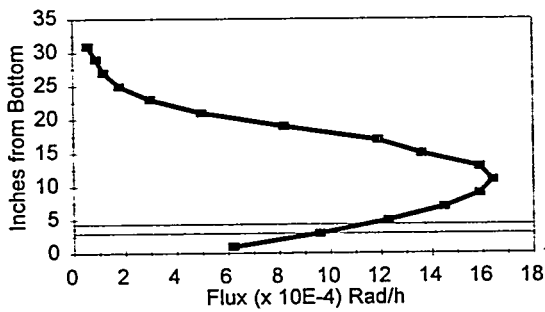
**Tube 20 (Sample 3)**



**Tube 11 (Sample 4)**



**Tube 21 (Sample 5)**



**Tube 22 (Sample 6)**

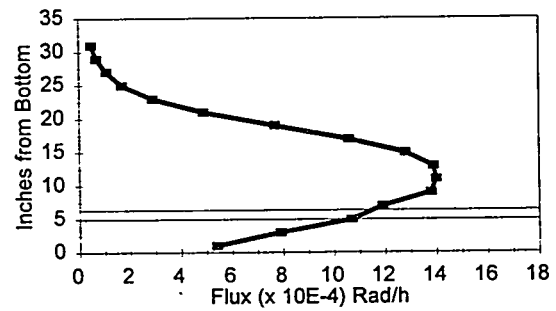
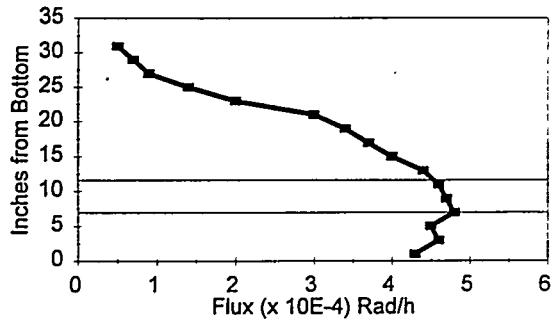
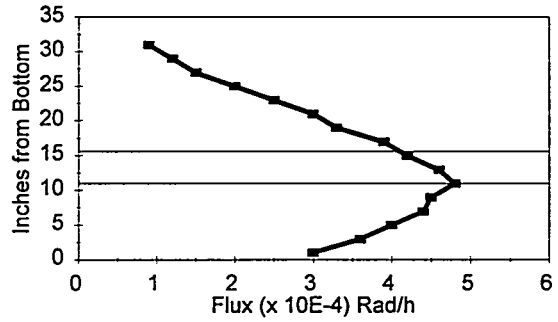


**Figure 2.1.** Gamma Dose Rate Cross Sections for Tubes Used in Hydrolysis Experiments Conducted at an Average of  $1.07 \times 10^5$  Rad/h

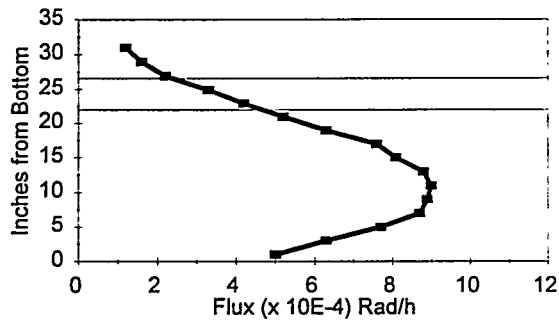
**Tube 4 (Sample 1)**



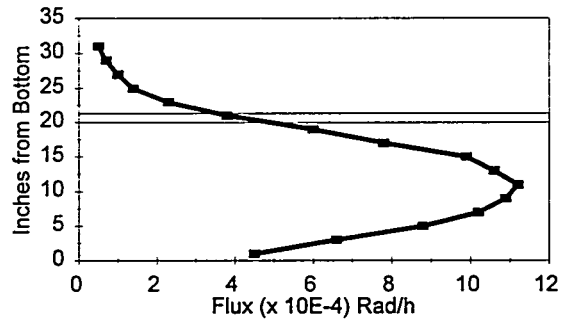
**Tube 15a (Sample 2)**



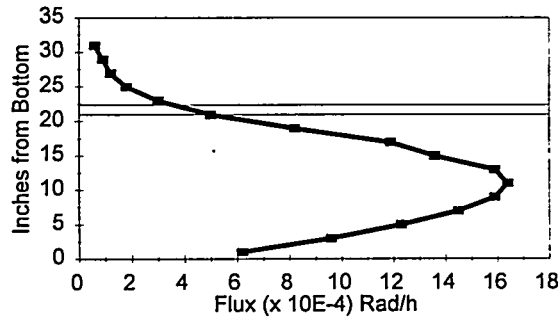
**Tube 15 (Sample 3)**



**Tube 20 (Sample 4)**



**Tube 21 (Sample 5)**



**Tube 22 (Sample 6)**

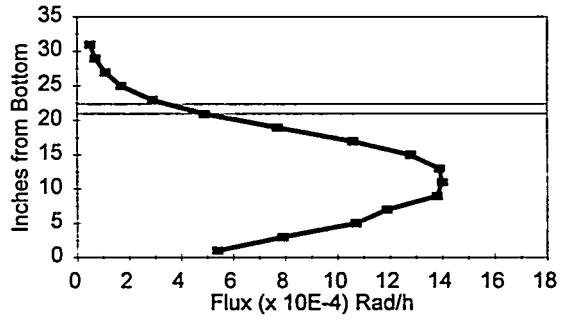
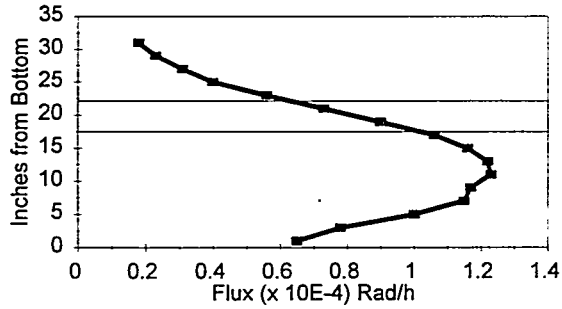
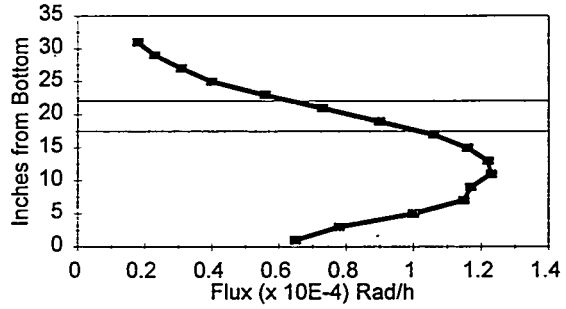


**Figure 2.2.** Gamma Dose Rate Cross Sections for Tubes Used in Hydrolysis Experiments Conducted at an Average of  $4.25 \times 10^4$  Rad/h

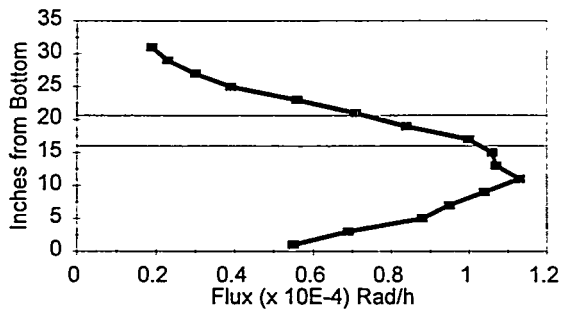
**Tube 24a (Sample 1)**



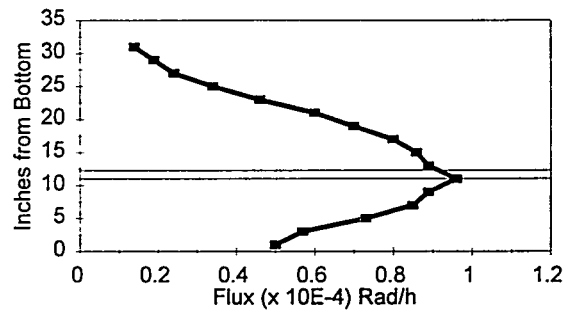
**Tube 24a (Sample 2)**



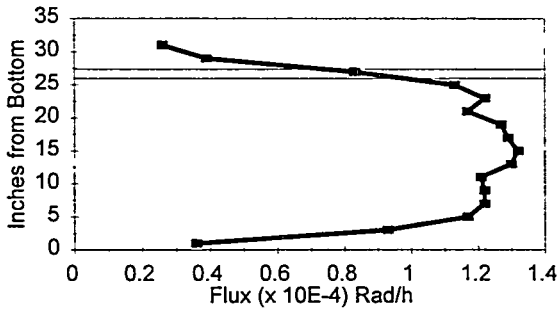
**Tube 23a (Sample 3)**



**Tube 25a (Sample 4)**



**Tube 8 (Sample 5)**



**Tube 23a (Sample 6)**

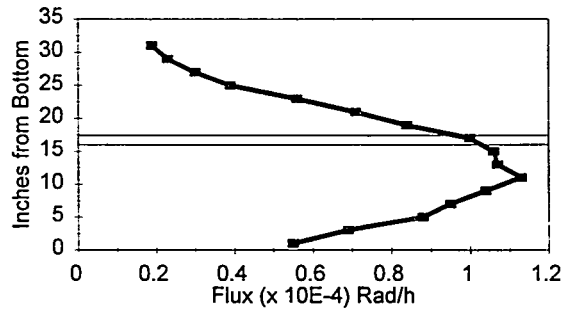


**Figure 2.3.** Gamma Dose Rate Cross Sections for Tubes Used in Hydrolysis Experiments Conducted at an Average of  $8.91 \times 10^3$  Rad/h

**Table 2.2.** Estimation of Integrated Gamma Dose in Hydrolysis Experiments at Various Dose Rates for the First and Last Samples Taken

Flux (Rad/h)	Integrated Gamma Dose (Rad)	
	Sample 1, 2 days	Sample 6, 19 days
$1.07 \times 10^5$	$5.1 \times 10^6$	$4.9 \times 10^7$
$4.25 \times 10^4$	$2.0 \times 10^6$	$1.9 \times 10^7$
$8.91 \times 10^3$	$3.9 \times 10^5$	$4.2 \times 10^6$

the calculated average gamma dose received by tank wastes, which is on the order of  $3 \times 10^7$  to  $5 \times 10^8$  Rad (Parra 1994). The gamma dose rate, of course, is much lower in the SSTs, currently ranging from about 20 to 200 Rad/h, than in these experiments ( $10^4$  to  $10^5$  Rad/h).

### 2.1.3 Analytical Methods

Several different analytical methods were used during the experiments. Gas samples from the headspace of the reaction vessels were obtained with an evacuated 75-mL sample vessel through a specially prepared gas sampling/pressure monitoring panel. The gas line on the panel leading to the sample vessel was evacuated prior to opening to the line connecting the panel to the reaction vessel. The sample vessel was equilibrated with the reaction vessel for 5 min before sealing. Gas samples were analyzed on a high-sensitivity Finnigan MAT-271 mass spectrometer for several gases, including argon, hydrogen, nitrogen, oxygen, and nitrogen oxides. The estimate of precision is better than 0.1 mole%.

Syringe-filtered supernates were analyzed by AA for total soluble iron, nickel, and cesium. These analyses are accurate to within 10%. Supernates were also analyzed for  $\text{NO}_3^-$ ,  $\text{NO}_2^-$ , and  $\text{HCO}_2^-$  by IC, which is accurate to 5%. Free  $\text{CN}^-$  ion was determined by IC and by ion selective electrode (ISE). The IC method for free  $\text{CN}^-$  ion was found to give inaccurate concentrations when solutions contained nickel cyanide complexes because of the use of ethylenediamine in the eluant, which releases nickel-bound cyanide. As discussed below, nickel was found to be redissolved in most of the reaction solutions, presumably as a cyanide complex. Therefore, the IC results were determined to be of no value in estimating the concentration of free  $\text{CN}^-$  ion as a reaction intermediate. Cyanide ion concentrations determined by ISE for selected reaction solutions are more reliable in this case because the analysis does not require dilution or addition of other reagents.

Dissolved ammonia was determined with use of an Orion 720A pH/ISE meter equipped with an Orion 95-12  $\text{NH}_3$  ISE. Before the reaction solution  $[\text{NH}_3]$  was determined, the accuracy of the ISE was checked using a standard  $\text{NH}_4\text{Cl}$  solution made basic by addition of an NaOH solution.

Calibration measurements were typically within 3% of the actual concentration (see below). Aluminum in reaction solutions was found to suppress the measured ammonia concentrations, as discussed in Section 2.5.

Gas-phase ammonia was estimated with use of GasTech ammonia sensing tubes. Tubes were connected to the reaction vessel with a gas-tight seal; the plunger on the supplied pump was pulled to the 50- or 100-mL position, drawing gas through the sensing tube. A color change in the sensing material indicates the presence of ammonia; the position of the line of demarcation between the reacted and unreacted sensing material indicates the concentration, which is read off the calibrated tube in ppm. The concentration was adjusted for the change in pressure that occurred when the volume was increased by pulling the plunger.

Experiments were performed to check the accuracy and suitability of the ISE method for dissolved ammonia analysis in which a known amount of  $\text{NH}_3$  was generated by adding various amounts of a standard 0.1 M  $\text{NH}_4\text{Cl}$  solution to 25 mL of 2 M  $\text{NaOH}$  in the reaction vessels. The range of ammonia concentrations generated was from 0.001 to 0.075 M, which encompasses the range of ammonia concentrations observed in the hydrolysis experiments (see Sections 2.3 through 2.5). Vessels were quickly sealed and heated to 90°C for 2 days without gamma irradiation. The vessels were cooled to room temperature and treated exactly like a vessel in a hydrolysis experiment; i.e., a 75-mL gas sample was taken (and later discarded), a gas sample was drawn through a GasTech ammonia sensing tube, and the vessel was sealed and returned to the laboratory for solution ammonia determination. As shown in Figure 2.4, the measured solution ammonia concentrations correlate well with the concentrations generated (data points); the least squares fit to the data (line) has a slope of 1.02 and intercept of 0.00. In addition, the number of moles of ammonia in the gas phase ( $10^{-8}$  to  $10^{-6}$  moles), as estimated with the GasTech sensor, was at least  $10^3$  times lower than the number of moles in solution ( $10^{-5}$  to  $10^{-3}$  moles). This ratio is consistent with that calculated using Henry's law (Edwards et al. 1978; Norton and Pederson 1994). These experiments demonstrate that ammonia concentrations can be accurately measured with the sampling scheme used; that adsorption of ammonia on the stainless steel vessel and tubing is not significant under the reaction and sampling conditions; and that the solution concentration, in solutions cooled to room temperature, adequately accounts for all ammonia generated from hydrolysis.

A similar set of experiments was conducted in which a known concentration of ammonia was generated from  $\text{NH}_4\text{Cl}$  and base, heated, and exposed to gamma radiation to investigate the behavior of ammonia in the gamma field. Six vessels were identically prepared containing 0.03 M  $\text{NH}_3$  (from  $\text{NH}_4\text{Cl}$ ), 2 M  $\text{NaOH}$ , 0.095 M  $\text{NaNO}_3$ , and 0.036 M  $\text{NaNO}_2$ . Nitrate and nitrite were added because they are nitrogen-containing species present in the IF-1B flowsheet material that undergo radiolysis. Concentrations of these species were chosen to mimic the concentrations present in IF-1B hydrolysis experiments. Each vessel was heated to 90°C; five were exposed to gamma radiation at a flux of  $1.07 \times 10^5$  Rad/h; and the sixth was not irradiated and served as a control. Vessels were individually pulled from the gamma tubes after 6, 8, 13, 17, and 20 days and analyzed. Two more controls were prepared containing 2 M  $\text{NaOH}$ , 0.095 M  $\text{NaNO}_3$ , and 0.036 M  $\text{NaNO}_2$  but no  $\text{NH}_3$  ( $\text{NH}_4\text{Cl}$ ). One was placed in a gamma tube, heated to 90°C, and irradiated at  $1.07 \times 10^5$  Rad/h, while the other

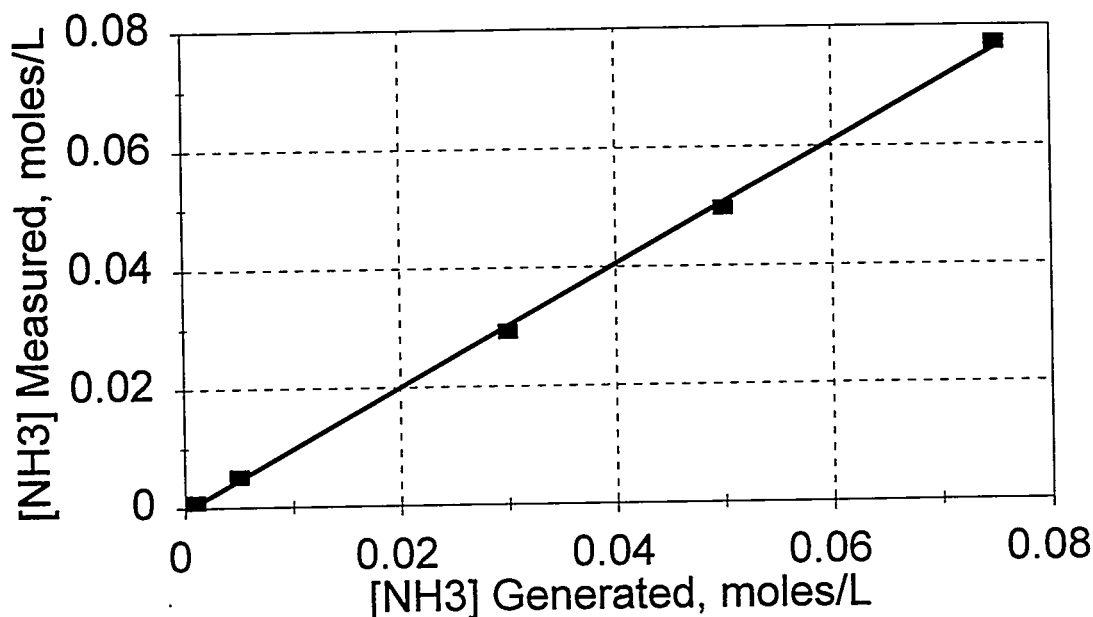


**Figure 2.4.** Measured Versus Generated Ammonia Concentration in Experiments Not Gamma Irradiated

received identical treatment but was not irradiated. The purpose of these two controls was to determine whether  $\text{NH}_3$  was generated radiolytically or thermally from nitrate or nitrite. All three controls were sampled after 20 days.

Results of this experiment are shown in Figure 2.5. The solution ammonia concentration is seen to decrease with time (data points shown), following zero-order behavior; i.e., the concentration decrease is linear with time. The least squares fit to the data (line shown) gives a rate constant for ammonia destruction of  $1.3 \times 10^{-3}$  moles/L/day at the applied dose rate of  $1.07 \times 10^5$  Rad/h. The zero-order behavior is consistent with rate-limiting radical (hydroxyl or oxide radical) formation, followed by more rapid reaction of the radical with  $\text{NH}_3$ . A different rate constant should be obtained at different dose rates; however, these rate constants have not yet been measured. The measured  $\text{NH}_3$  concentration in the control vessel containing  $\text{NH}_3$  but not subjected to irradiation was 0.029 M, the same as the starting concentration within experimental error. No ammonia was generated in either of the two controls not initially containing  $\text{NH}_3$ , indicating that  $\text{NH}_3$  is not generated from nitrate or nitrite under the conditions of the IF-1B hydrolysis experiments.

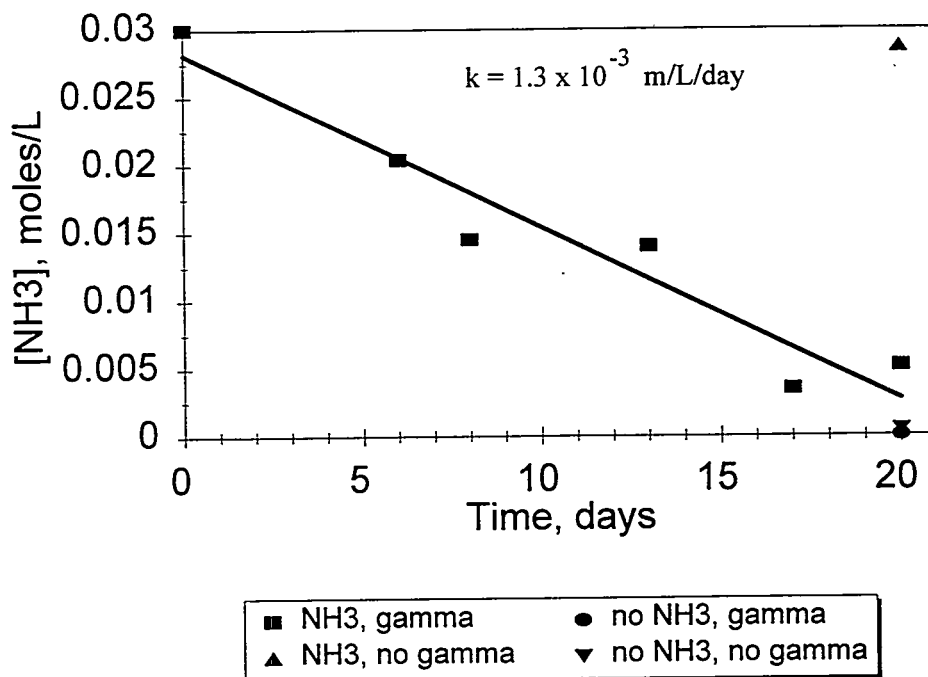


Figure 2.5. Ammonia Concentration as a Function of Time Irradiated at a Gamma Dose Rate of  $1.07 \times 10^5$  Rad/h

## 2.2 Cesium Ion Exchange in Competition with Ferrocyanide Dissolution

In waste processing operations at Hanford, ferrocyanides were precipitated to scavenge cesium; supernates were pumped off; and new waste was added on top of the ferrocyanide bed. The waste added was often highly caustic and also contained cesium. For example, neutralized current acid waste contained about 5 Ci/L  $^{137}\text{Cs}$ . If about 40% of the cesium was present as  $^{137}\text{Cs}$ , the total cesium concentration was on the order of  $1 \times 10^{-3} M$  when added to the tanks. Assuming the waste contacted the ferrocyanide sludge, both dissolution and ion exchange processes could have occurred.

In previous solubility studies (Bryan et al. 1993; Lilga et al. 1993), a material containing  $\text{Cs}_2\text{NiFe}(\text{CN})_6$  (PNL-prepared FECN-14, prepared in the absence of sodium ion) was found to be insoluble in up to 4 M NaOH at room temperature. Also, In-Farm-1A, Rev. 4 (IF-1A), which contains cesium, dissolved to a lesser extent and at a slower rate than the so-called "Vendor" ferrocyanide material,  $\text{Na}_2\text{NiFe}(\text{CN})_6 \cdot \text{Na}_2\text{SO}_4 \cdot 4.5 \text{H}_2\text{O}$ , which does not contain cesium. Apparently, as the  $\text{Na}_2\text{NiFe}(\text{CN})_6$  in the IF-1A material dissolves, cesium becomes concentrated at the particle surface to form an insoluble cesium-rich phase, inhibiting dissolution. The actual chemical composition of the cesium-rich phase and the solubility of mixed Cs/Na phases, such as  $\text{NaCsNiFe}(\text{CN})_6$ , have not been determined.

Solid sodium nickel ferrocyanide materials are also known to be excellent ion exchange materials for cesium (Loewenschuss 1982; Loos-Neskovic and Fedoroff 1989; Loos-Neskovic et al. 1976, 1990). Selectivity for cesium over sodium is very high (Campbell et al. 1990; Loos-Neskovic et al. 1976).

The extent of these two processes depends on their relative rates and the amount of mixing that occurred. If cesium uptake is relatively fast, all of the cesium could ion-exchange before the ferrocyanide exposed to the waste dissolves. If dissolution is fast relative to ion exchange, some of the cesium could be left in solution.

In the work conducted here, competition experiments were used to provide an indication of the rate of ion exchange relative to the rate of dissolution. Two room-temperature experiments exploring Vendor material dissolution (1 g) were conducted in the presence of  $2.3 \times 10^{-3} M$   $CsNO_3$  (50 mL), one containing 3 M NaOH, the other containing 4 M NaOH (typical concentrations for solutions from the evaporator). The NaOH solution containing cesium was added to the solid Vendor material then stirred, and solution samples were periodically taken and analyzed for soluble iron (ferrocyanide anion) and cesium ion by AA. The results of both of these experiments were very similar, indicating an insensitivity to base strength, as illustrated in Figure 2.6. Dissolution, as determined by the soluble iron, was 70% to 80% complete within 2 min, reaching 85% to 90% after 24 h. Cesium uptake was also very rapid with 98% incorporation into the solid phase after 2 min when the first solution sample was taken.

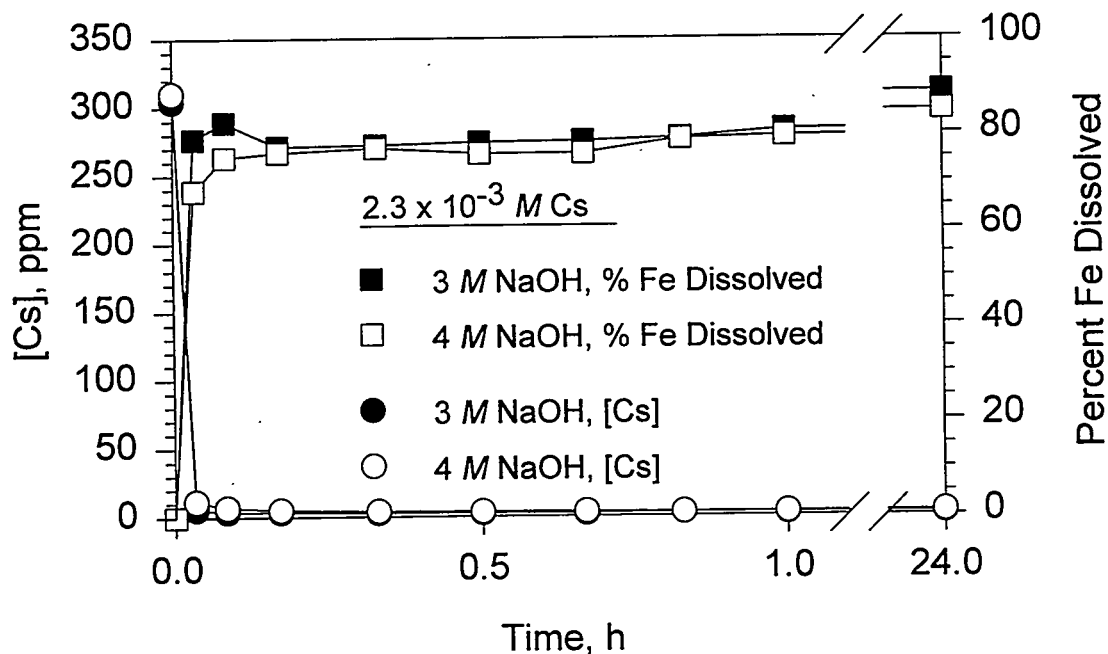


Figure 2.6. Dissolution and Cesium Ion Exchange in 3 and 4 M NaOH at an Initial [Cs] of  $2.3 \times 10^{-3} M$

Figure 2.7 compares results of experiments conducted in 4 M NaOH with either  $3 \times 10^{-4}$  or  $2.3 \times 10^{-3}$  M cesium ion. Less dissolution is observed at the higher cesium concentration, with about 10% less dissolution under these conditions. At the higher cesium concentration, more cesium incorporation occurs, forming more of the insoluble cesium-containing ferrocyanide phase. The number of moles of cesium in 50 mL of the  $3 \times 10^{-4}$  M solution was not enough to measurably decrease the ferrocyanide solubility, showing essentially the same dissolution behavior as the Vendor material in the absence of cesium ion. The [Cs] is quickly reduced to the AA detection limit for both of the starting concentrations tested.

These experiments using the Vendor ferrocyanide simulant, which does not initially contain cesium, can be compared with dissolution experiments of the IF-1A flowsheet simulant, which was precipitated with cesium. Figure 2.8 illustrates the difference in dissolution behavior between the Vendor material in the presence of soluble cesium and the IF-1A material containing cesium already incorporated in the solid phase. Cesium in the solid phase inhibits dissolution, making dissolution of the In-Farm material slow relative to materials not initially containing cesium. Dissolution of the Vendor material is not inhibited initially and dissolution is rapid. However, because cesium ion exchanges into the solid phase, dissolution slows and becomes incomplete. The rate of cesium ion exchange is apparently faster than the rate of ferrocyanide dissolution since cesium is effectively removed from solution before dissolution is complete.

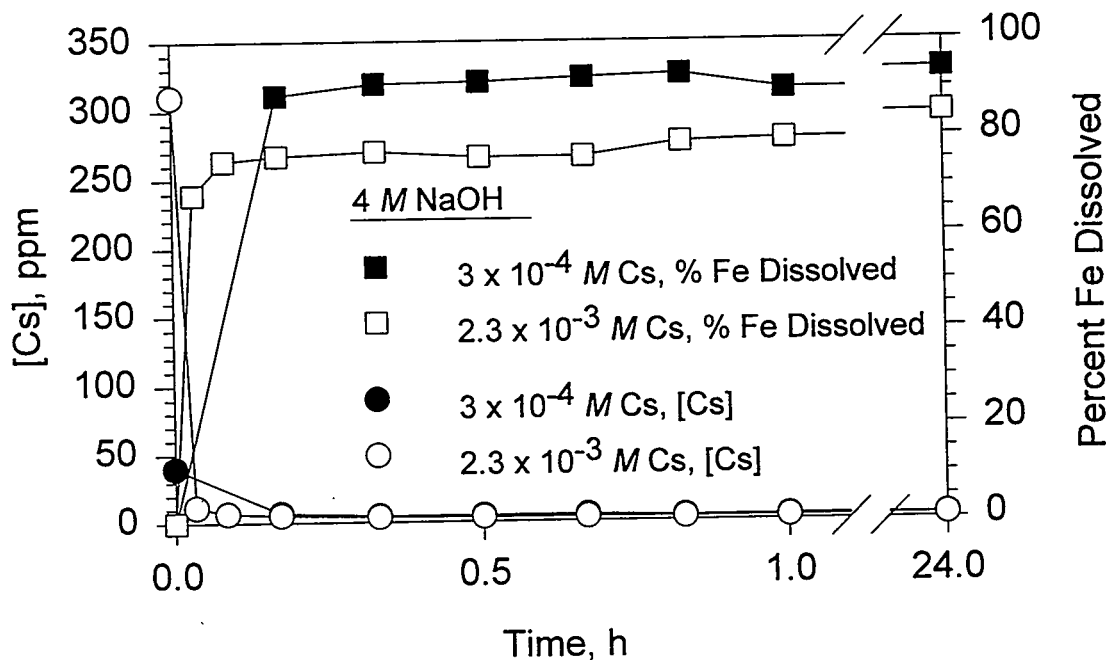
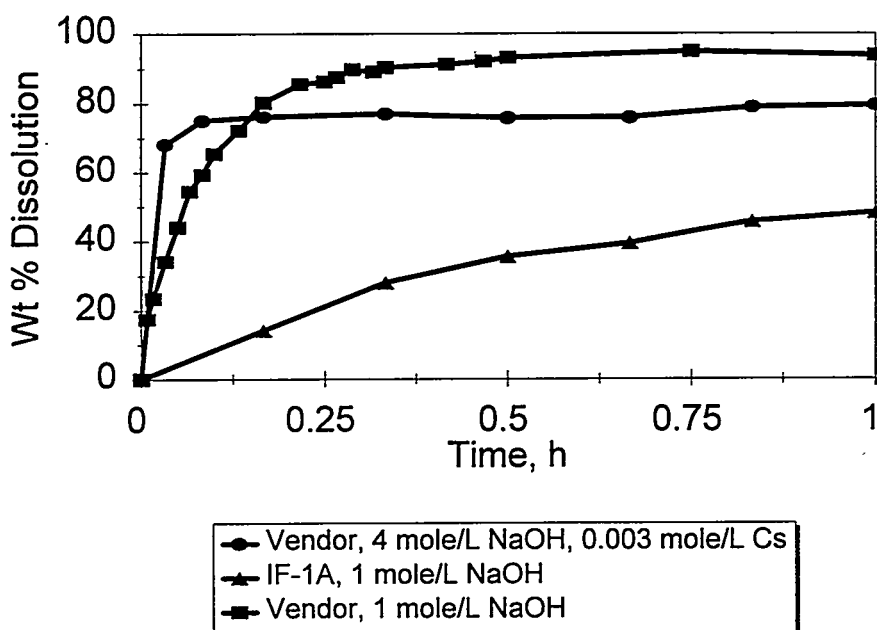


Figure 2.7. Dissolution and Cesium Ion Exchange in 4 M NaOH at  $2.3 \times 10^{-3}$  M and  $3 \times 10^{-4}$  M Initial Cesium Ion Concentration



**Figure 2.8.** Dissolution Behavior of a Solid In-Farm Flowsheet Material Containing Cesium Ion Compared with a Solid Vendor-prepared Simulant Not Containing Cesium

In addition, more insoluble ferrocyanide is present at the end of these experiments than might be predicted from the number of moles of cesium present. For a  $\text{Cs}_2\text{NiFe}(\text{CN})_6$  phase, the Fe/Cs mole ratio would be 0.5; for a  $\text{CsNaNiFe}(\text{CN})_6$  phase, this ratio would be 1.0. For IF-1A dissolution, the Fe/Cs mole ratio was found to be 3.3 (although dissolution may not have reached equilibrium at the end of this experiment, in which case, the ratio would be smaller). For the Vendor material dissolutions, this ratio varied from 1.4 to about 8. These results are consistent with the formation of an insoluble cesium-rich ferrocyanide phase at the particle surface, encasing otherwise-soluble  $\text{Na}_2\text{NiFe}(\text{CN})_6$ .

### 2.3 Hydrolysis of In-Farm Ferrocyanide Flowsheet Material in 2 M NaOH

Several experiments were conducted in 2 M NaOH solution to investigate the influence of gamma dose rate, temperature, and initial ferrocyanide anion concentration (i.e., the portion of the ferrocyanide in the IF-1B simulant that is soluble under these conditions; see Table 2.1) on the hydrolysis of IF-1B flowsheet material. Table 2.3 outlines the conditions used in the hydrolysis experiments. The first row of Table 2.3 shows base values of parameters ( $1.07 \times 10^5$  Rad/h, 0.5 g IF-1B,  $90^\circ\text{C}$ ); experiments investigating variation of one parameter (column) were conducted using the base values of the other two parameters.

**Table 2.3.** Ferrocyanide Hydrolysis Variables Investigated

<u>Gamma Field (Rad/h)</u>	<u>Weight IF-1B Flowsheet Material (g)</u>	<u>Temperature (°C)</u>
1.07 x 10 <sup>5</sup>	0.5	90
4.25 x 10 <sup>4</sup>	0.25	70
8.91 x 10 <sup>3</sup>	1	50

All of the experiments discussed in this section were conducted in 2 M NaOH. The base concentration was not varied because it has been reported that the rate of thermal ferrocyanide hydrolysis is independent of hydroxide ion concentration above pH 10 (Robuck and Luthey 1989). For experiments reported in this section, the hydrolysis reaction conducted in a gamma field was also assumed to be zero-order in hydroxide ion concentration. Although hydroxide ion is consumed to precipitate nickel and iron, hydroxide ion is present in large excess. Experiments conducted at pH 10 are discussed in Section 2.4.

### 2.3.1 Dependence of Hydrolysis on Temperature

Table 2.4 summarizes conditions of experiments in which temperature was the investigated variable. The temperature range of 50°C to 90°C was chosen to represent present and past conditions in the tanks. Figure 2.9 shows ammonia and formate produced by hydrolysis in the gamma-irradiated and thermal (control) experiments at 90°C (H1). Gamma radiation promotes the hydrolysis reaction, as illustrated most clearly by the ammonia data. About 10 times more ammonia was produced after 12 days in the gamma field than in the identical, but non-irradiated, control. This ratio is somewhat less after 19 days because, in the gamma field, NH<sub>3</sub> is destroyed, leading to a flattening-out of the NH<sub>3</sub> production curve. As will be seen, this leveling or even decreasing [NH<sub>3</sub>] after long reaction times is a typical feature of much of the following data, but does not necessarily represent the approach to

**Table 2.4.** Conditions for IF-1B Hydrolysis Experiments Investigating the Effect of Temperature Variation. Experiments were conducted in 25 mL of 2 M NaOH for 3 weeks.

<u>Experiment Number</u>	<u>Gamma Dose Rate (Rad/h)</u>	<u>Weight IF-1B used (g)</u>	<u>Temperature (°C)</u>
H1	1.07 x 10 <sup>5</sup>	0.5	90
H2	1.07 x 10 <sup>5</sup>	0.5	70
H3	1.07 x 10 <sup>5</sup>	0.5	50

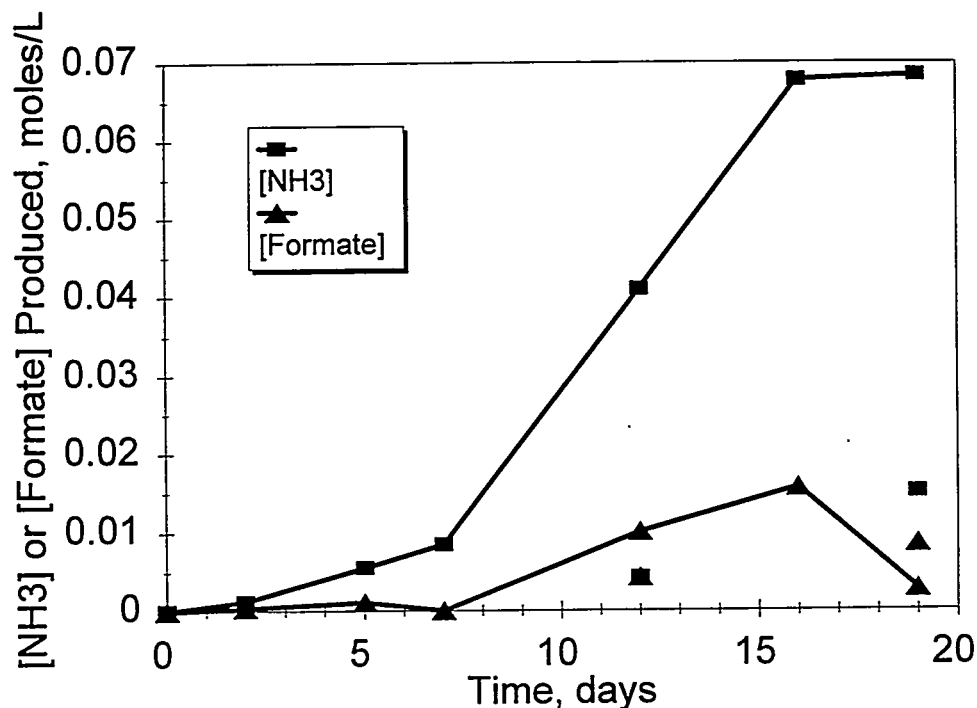


**Figure 2.9.** Ammonia and Formate Ion Production in the Hydrolysis of IF-1B in 2 M NaOH at 90°C and  $1.07 \times 10^5$  Rad/h (H1). Control experiments were identical but not irradiated.

complete ferrocyanide destruction. This behavior is more often an indication of the relative rate of ammonia production versus the rate of ammonia destruction in the gamma field. For experiment H1, however, the amount of ammonia in solution after 19 days represents at least 90% ferrocyanide destruction, not taking into account the amount of ammonia destroyed.

Other typical features of ammonia generation illustrated by the H1 data are the relatively long induction period of about 7 days and the ensuing period of more rapid  $\text{NH}_3$  production. The sigmoidal shape and the long induction period suggest the possibility that relatively inactive intermediates, formed after some fraction of cyanide is liberated and hydrolyzed, are slowly converted to more reactive cyanide complexes. The reaction mechanism is complex and likely involves pre-equilibria and possibly the formation of dimeric or higher iron cyanide clusters and nickel cyanide complexes (see below).

Formate is also a product of cyanide ion hydrolysis, 1 mole being formed for each mole of ammonia produced. The one-to-one stoichiometry is approximated in the H1 control experiments (Figure 2.9), which were not irradiated. Figure 2.9 shows that the formate ion concentration during the course of the experiment parallels ammonia production; an induction period, a period of more rapid

formate ion formation (increasing formate ion concentration), and a period of decreasing formation rate (decreasing formate ion concentration) are seen. The formate ion concentration is about five times less than that of ammonia and decreases rapidly near the end of the experiment because it is destroyed in the gamma field (Goldstein et al. 1988). These results suggest that formate ion is destroyed more efficiently in the gamma field than is ammonia, but the rate of destruction has not yet been experimentally determined under the conditions used in this research. No formate ion could be detected in any of the 50°C and 70°C reaction solutions, including controls, consistent with the low extent of ammonia production at these temperatures.

Figure 2.10 and an expanded view of the ammonia production data in Figure 2.11 show the strong temperature dependence of the hydrolysis reaction in this temperature range. At 70°C, conversion to ammonia in the gamma field is only about two to four times that in the thermal controls. This ratio drops to less than 2 at 50°C. Data at the lower temperatures do not show the sigmoidal character because the conversion is very low. The strong temperature dependence indicates that even though a gamma-enhanced process is occurring, a thermally controlled reaction is important in determining the rate and extent of reaction. It is possible that this thermal process involves cyanide dissociation from the iron center (a reversible process).

The change in soluble iron concentration (as determined by AA) for experiment H1 is shown in Figure 2.12. The observed data, shown as data points, are a measure of all soluble iron species including, but not limited to, the  $\text{Fe}(\text{CN})_6^{4-}$  anion. Other soluble species that could be present include iron cyanides that contain less than six cyanide ligands per metal ion or metal cluster complexes. For an unknown reason, the iron concentration measured in the solution removed on Day 2 (0.0197 M) was higher than that expected for dissolution of the IF-1B material in 2 M NaOH (0.0127 M). The line in the figure represents a first-order fit to all of the data, the rate constant of 0.17 day<sup>-1</sup> being determined from the slope of the line in a plot of  $\ln[\text{Fe}]$  versus time (Figure 2.13). The rate constant is a pseudo-first-order rate constant since the loss of soluble iron from solution likely involves reaction with hydroxide, present in large excess, to precipitate iron hydroxides or oxides. The iron concentrations in experiments H2 and H3 did not decrease below the expected initial concentration, which is consistent with the very low ammonia production.

The changes in nitrate and nitrite concentrations and the sum of these two concentrations for Experiment H1 are shown in Figure 2.14. These data are also representative of changes observed in all other hydrolysis experiments. In a typical hydrolysis experiment, dissolution of 0.5 g of the dried IF-1B flowsheet material gave a solution with an initial  $[\text{NO}_2^-]$  of 0.030 M and an initial  $[\text{NO}_3^-]$  of 0.10 M. Nitrate ion concentrations decreased and nitrite ion concentrations increased during the course of each hydrolysis experiment in the gamma field. However, the sum of these concentrations is about constant for each series of experiments. These results were also seen in FY 1993 research. For controls in each series of experiments (data points not connected with a line in Figure 2.14) that were not irradiated, both nitrate and nitrite ion concentrations remained largely unchanged from the starting concentrations.

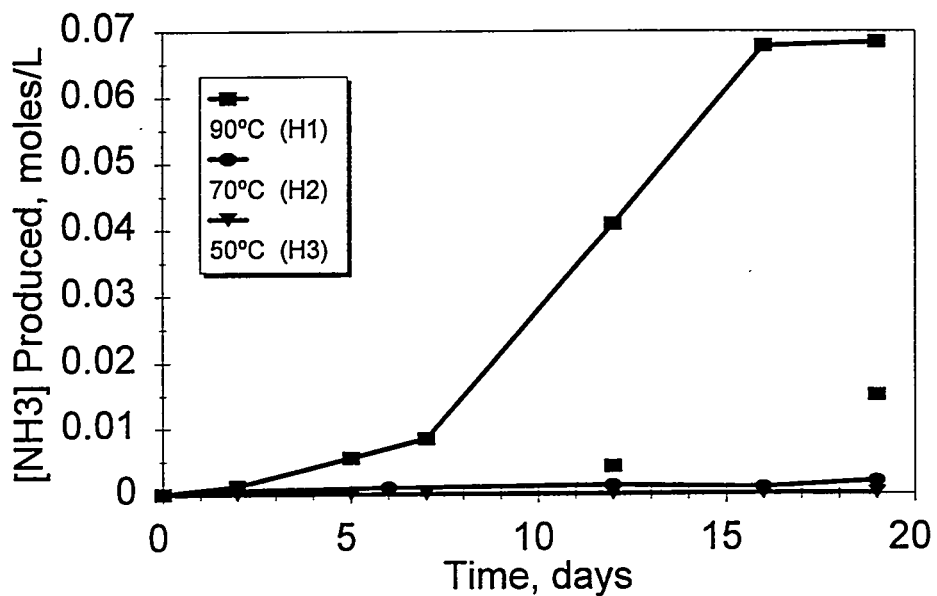


Figure 2.10. Temperature Dependence of Ammonia Production in the Hydrolysis of IF-1B (0.5 g) at a Gamma Dose Rate of  $1.07 \times 10^5$  Rad/h (H1)

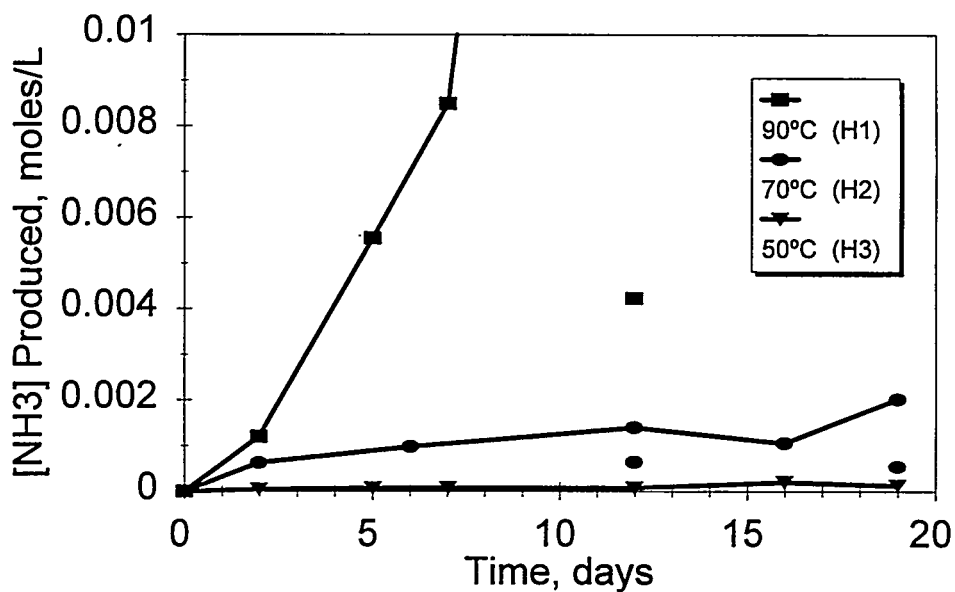


Figure 2.11. Temperature Dependence of Ammonia Production in the Hydrolysis of IF-1B (0.5 g) at a Gamma Dose Rate of  $1.07 \times 10^5$  Rad/h (H1), Expanded View

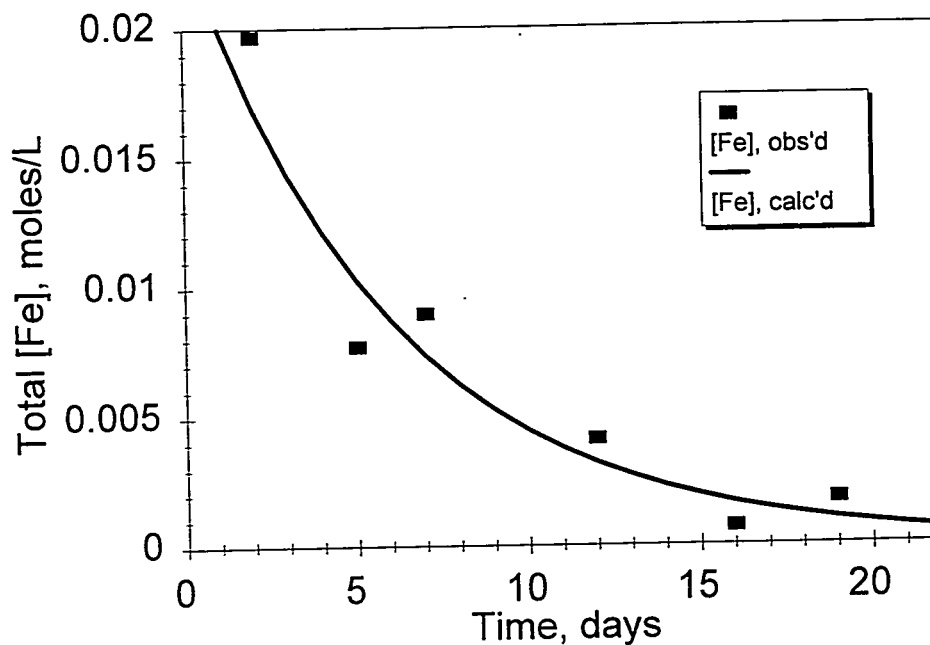


Figure 2.12. Total Iron Concentration in the Hydrolysis of IF-1B (0.5 g) at 90°C and at a Gamma Dose Rate of  $1.07 \times 10^5$  Rad/h (H1)

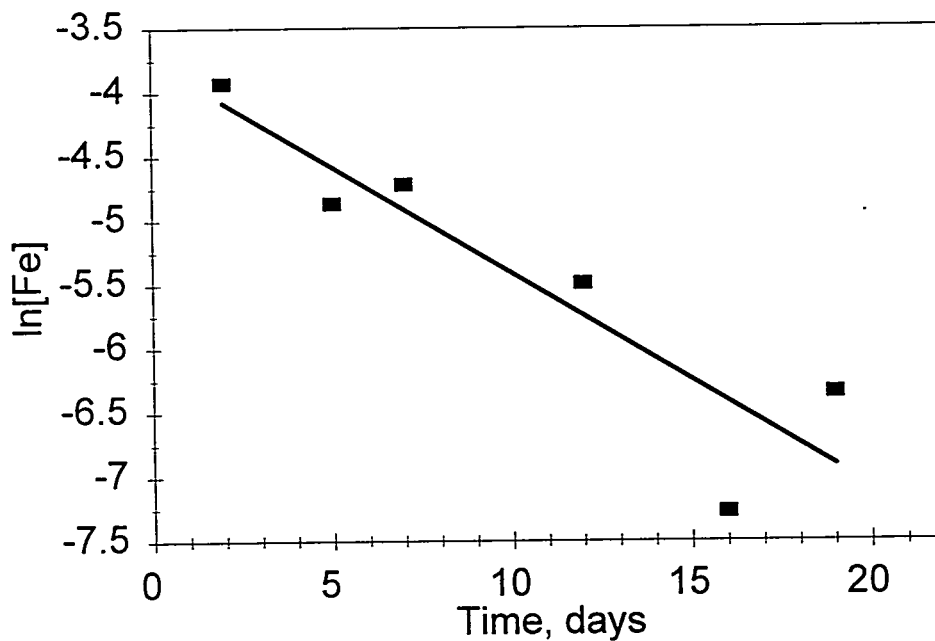
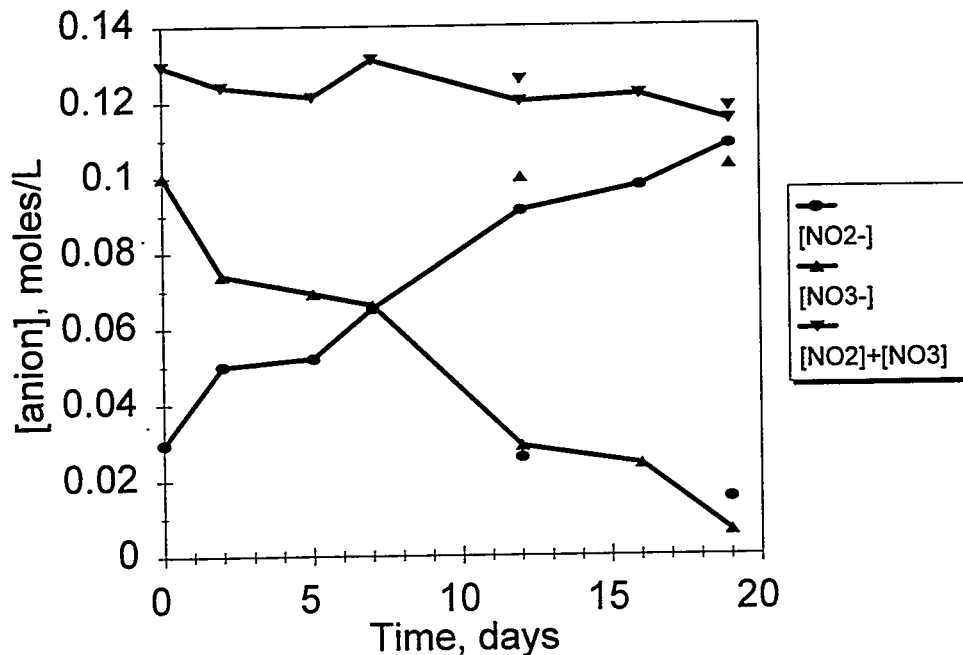


Figure 2.13. First-order Plot for the Change in Iron Concentration in the Hydrolysis of IF-1B (0.5 g) at 90°C and at a Gamma Dose Rate of  $1.07 \times 10^5$  Rad/h (H1)



**Figure 2.14.** Changes in Nitrate and Nitrite Ion Concentrations and the Sum of These Concentrations in the Hydrolysis of IF-1B (0.5 g) at 90°C and at a Gamma Dose Rate of  $1.07 \times 10^5$  Rad/h (H1)

In the gamma field, nitrate destruction and nitrite formation followed zero-order kinetics; plots of concentration versus time are linear, as shown in Figures 2.15 and 2.16. Linear regression of the data (lines drawn through the data points) give the rate constants shown in Table 2.5. The rate of nitrate ion destruction equals the rate of nitrite ion formation, suggesting conversion of nitrate to nitrite. The calculated activation energies for nitrate destruction and for nitrite formation are 32 kJ/mole and 28 kJ/mole, respectively.

The soluble nickel concentrations for samples from Experiment H1 are shown in Figure 2.17. The nickel concentration increased to a maximum on Day 12, representing 92 mole% of the nickel initially precipitated as  $\text{Ni}(\text{OH})_2$  when IF-1B was contacted with 2 M NaOH. It is likely that nickel is resolubilized by cyanide ion liberated as an intermediate during ferrocyanide hydrolysis. The feasibility of this behavior was demonstrated in separate control experiments in which nickel from  $\text{Ni}(\text{OH})_2$  was redissolved when aqueous 2 M NaOH solutions containing cyanide ion at concentrations ranging from 0 to 0.1 M were added and stirred. Confirmation of the identity of the nickel cyanide complex [most likely  $\text{Ni}(\text{CN})_4^{2-}$ ] awaits the infrared spectroscopic analysis of reaction solutions planned for FY 1995.

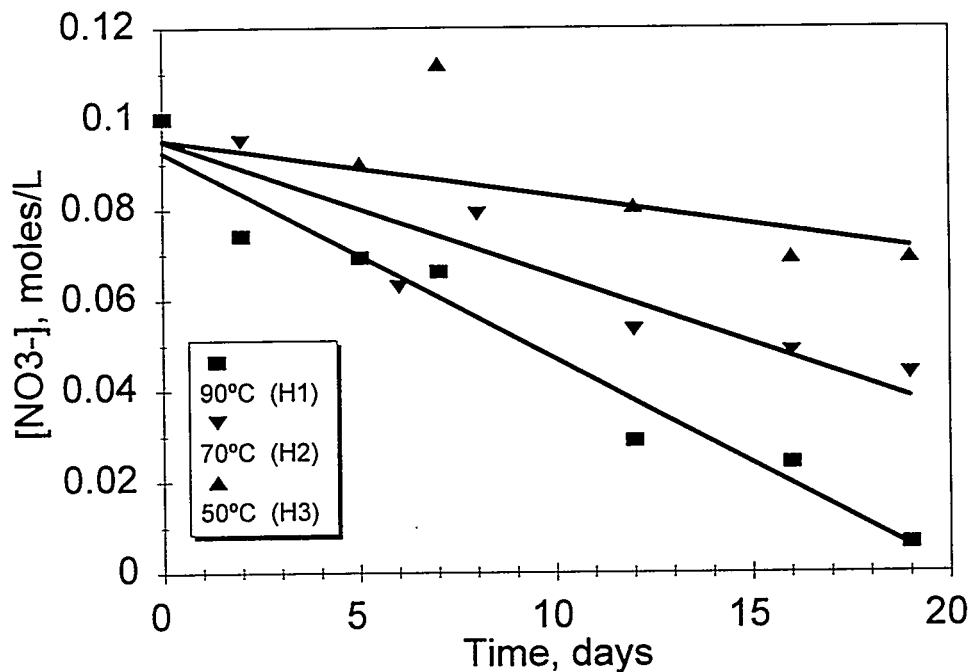


**Figure 2.15.** Temperature Dependence of Nitrate Destruction in the Hydrolysis of IF-1B (0.5 g) at a Gamma Dose Rate of  $1.07 \times 10^5$  Rad/h. Measured concentrations (data points) and zero-order fit (lines) are shown.

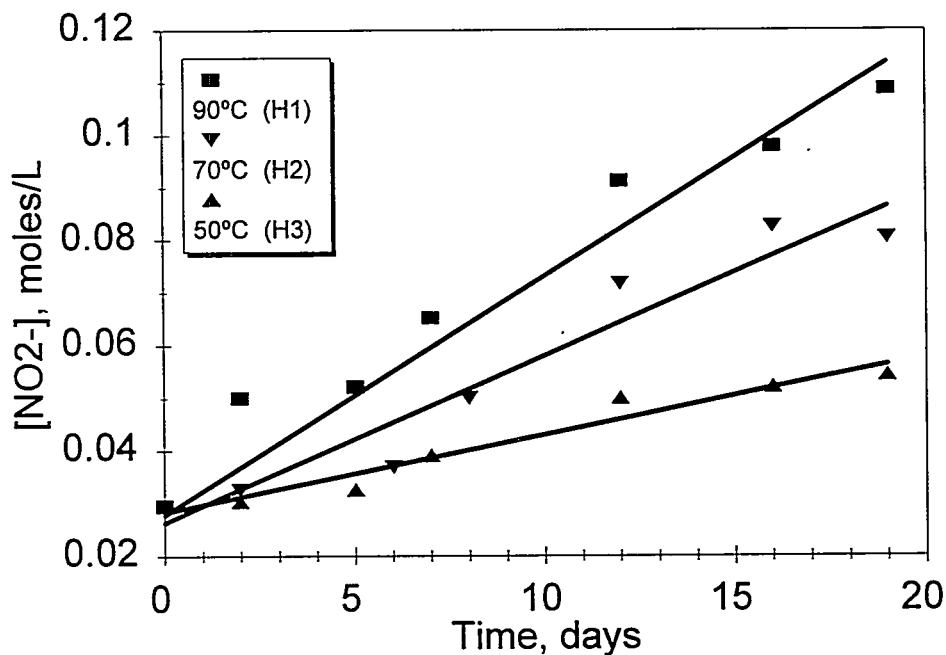


**Figure 2.16.** Temperature Dependence of Nitrite Formation in the Hydrolysis of IF-1B (0.5 g) at a Gamma Dose Rate of  $1.07 \times 10^5$  Rad/h. Measured concentrations (data points) and zero-order fit (lines) are shown.

Table 2.5. Rate Constants for Nitrate Destruction and Nitrite Formation at Various Temperatures

Experiment Number	Temperature (°C)	NO <sub>2</sub> <sup>-</sup> Formation Rate Constant (moles/L/day)	NO <sub>3</sub> <sup>-</sup> Destruction Rate Constant (moles/L/day)
H1	90	4.5 x 10 <sup>-3</sup>	4.6 x 10 <sup>-3</sup>
H2	70	3.2 x 10 <sup>-3</sup>	3.0 x 10 <sup>-3</sup>
H3	50	1.5 x 10 <sup>-3</sup>	1.2 x 10 <sup>-3</sup>

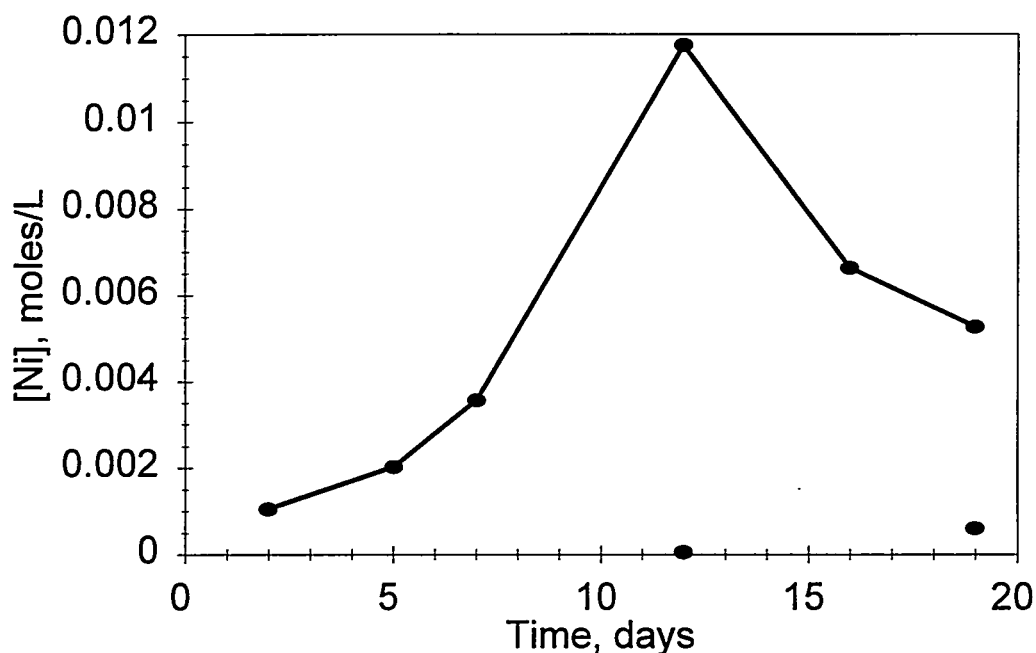
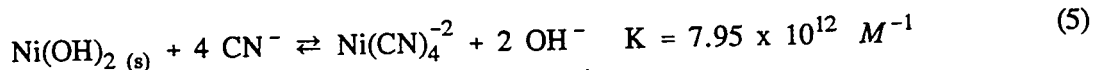


Figure 2.17. Total Nickel Concentration in the Hydrolysis of IF-1B (0.5 g) at 90°C and at a Gamma Dose Rate of 1.07 x 10<sup>5</sup> Rad/h (H1)

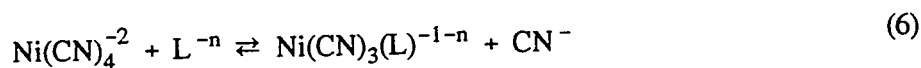
Cyanide redissolution of Ni(OH)<sub>2</sub> is consistent with known equilibrium data (Butler 1964; Christensen et al. 1963). Equations (3) through (5) indicate that the formation of Ni(CN)<sub>4</sub><sup>-2</sup> should be highly favored even in solutions containing several orders of magnitude more hydroxide ion than

cyanide ion. Using these reported equilibrium data, the overall equilibrium constant for the formation of  $\text{Ni}(\text{CN})_4^{-2}$ , Eq. (5), was calculated to be  $7.95 \times 10^{12} \text{ M}^{-1}$ .



Analyses of the free cyanide ion concentration were attempted using IC. However, it was later found that ethylenediamine was used in the IC method; ethylenediamine is reported to displace about 80% of the cyanide bound to nickel (Rocklin and Johnson 1983). Free cyanide ion concentrations, as determined by IC, in the nickel redissolution control experiments are an order of magnitude larger than expected from equilibrium data. The observed concentrations can be rationalized by assuming 60% displacement of nickel-bound cyanide under the analysis conditions used, in good agreement with the literature.

More realistic concentrations are provided by ISE, which does not require dilution or sample pretreatment. Equilibrium free cyanide ion concentrations for the nickel redissolution control experiments, determined by ISE without dilution, are shown in Figure 2.18. These data are consistent with free cyanide ion, possibly displaced by hydroxide or water (L), in equilibrium with a nickel-cyanide complex. Such an equilibrium has the general form of Eq. (6), in which the  $\text{Ni}(\text{CN})_4^{-2}$  is assumed to be the nickel-cyanide complex. If the total nickel concentration is much greater than the free cyanide ion concentration (a valid assumption), the equilibrium constant is predicted to be proportional to  $[\text{CN}^-]^2/[\text{Ni}]$ . Figure 2.19 shows that this relationship holds. Identification of the nickel-cyanide complex and the displacing ligand requires further investigation, such as by spectroscopic analysis.



### 2.3.2 Dependence of Hydrolysis on Gamma Dose Rate

Gamma dose rate was varied over one order of magnitude in the three sets of experiments conducted. Dose rates used were higher than those experienced by waste in SSTs, but the integrated dose was about the same (see Section 2.1.2). Table 2.6 summarizes the gamma dose rates used and other conditions of each experiment.

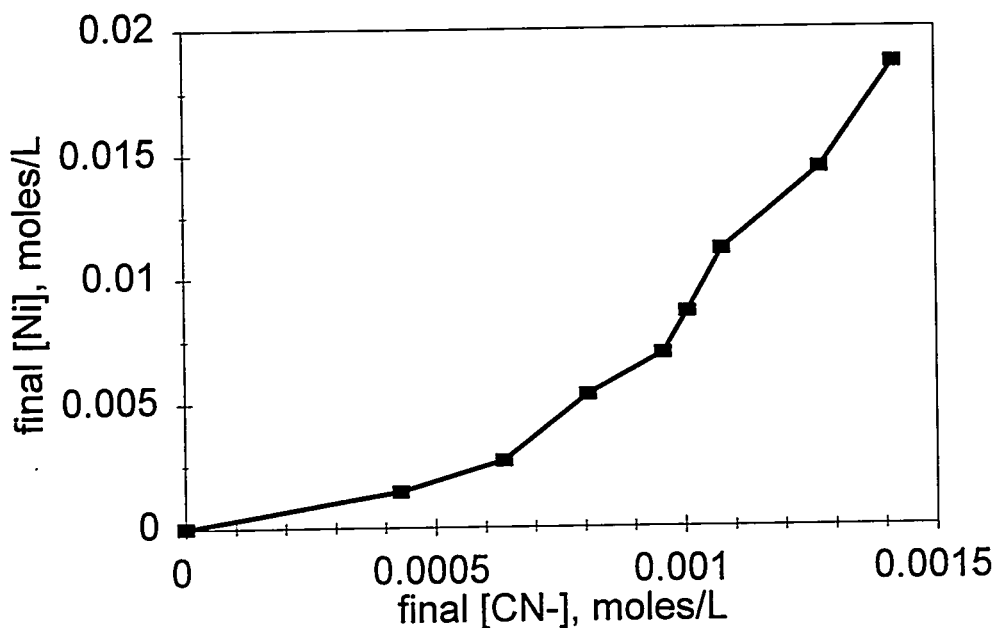


**Figure 2.18.** Equilibrium Free Cyanide Ion Versus Nickel Concentrations for the Nickel Redissolution Control Experiments Determined by Ion Selective Electrode

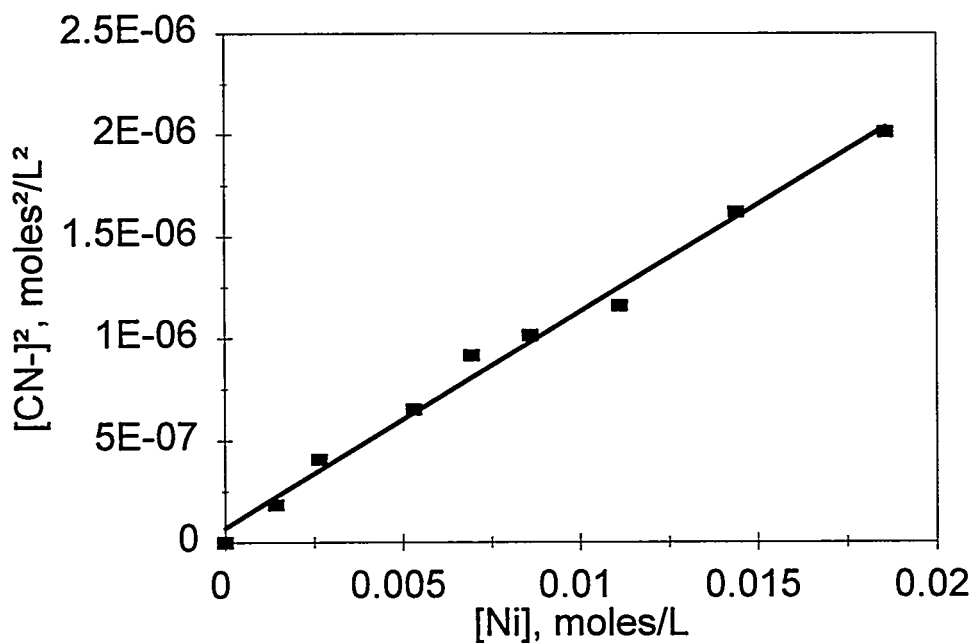


**Figure 2.19.** Plot of  $[\text{CN}^-]^2$  Versus  $[\text{Ni}]$  for Nickel Redissolution Control Experiments at Equilibrium. Data points and linear regression shown.

**Table 2.6.** Conditions for IF-1B Hydrolysis Experiments Investigating the Effect of Gamma Dose Rate Variation. Experiments conducted in 25 mL of 2 M NaOH for 3 weeks.

<u>Experiment Number</u>	<u>Gamma Dose Rate (Rad/h)</u>	<u>Weight IF-1B used (g)</u>	<u>Temperature (°C)</u>
H1	$1.07 \times 10^5$	0.5	90
H4	$4.25 \times 10^4$	0.5	90
H5	$8.91 \times 10^3$	0.5	90

At each dose rate, conversion was enhanced by the gamma field as compared with the thermal controls, as previously seen. At Day 12, the amount of ammonia produced in solutions irradiated at  $4.25 \times 10^4$  Rad/h (H4) and  $8.91 \times 10^3$  Rad/h (H5) was about 11 and 8 times more, respectively, than in the associated controls. Conversions in controls for H1, H4, and H5 were comparable.

The influence of dose rate on production of  $\text{NH}_3$  is shown in Figure 2.20. As dose rate decreases, the rate of  $\text{NH}_3$  production also decreases. The ammonia concentration in Experiment H5 decreased slightly after 16 days of reaction, indicating the rate of ammonia production was less than the rate of its destruction. The concentration in solution on Day 16 only accounts for, on the average, about one cyanide hydrolyzed per ferrocyanide anion added, not considering the amount of ammonia destroyed.

Figure 2.21 plots the observed ammonia concentrations as a function of integrated dose (Rad). Although lower dose rates lead to slower conversion to ammonia compared with higher dose rates, production of ammonia is apparently more efficient than ammonia destruction. Decreasing the hydroxyl or oxide radical concentration (by decreasing the dose rate) may decrease the rate of ammonia destruction more than the rates of hydrolysis processes.

Formate concentrations are shown in Figure 2.22 for hydrolyses conducted in the presence of gamma radiation at dose rates of  $5 \times 10^4$  Rad/h (H4) and  $1 \times 10^4$  Rad/h (H5). As seen in the experiment at  $1.07 \times 10^5$  Rad/h (H1), formate production parallels ammonia production, but the concentration of formate is less than that of ammonia. The disparity in concentrations is greater at higher dose rates. For example, at  $1.07 \times 10^5$  Rad/h (H1),  $[\text{NH}_3]/[\text{HCO}_2^-]$  is typically on the order of about 4. At  $4.25 \times 10^4$  Rad/h (H4), this ratio varies from about 1.5 to 3.8, and at  $8.91 \times 10^3$  Rad/h (H5), this ratio is between 1 and 1.5 for most samples. Both species are destroyed in the gamma field, but formate is destroyed faster and is more sensitive to increasing dose rates.

The relatively low extent of hydrolysis at the lowest dose rate (H5) is consistent with the observation that the concentration of soluble iron species does not change as a function of reaction time over the 3-week duration of the experiment (Figure 2.23), remaining essentially the same as that expected to be present initially. The solution iron profile for H4 is different, showing that the concentration remains constant for at least 7 days, then falls off. The drop in soluble iron corresponds to the period of more rapid ammonia and formate formation. Apparently, as cyanide ion is hydrolyzed,

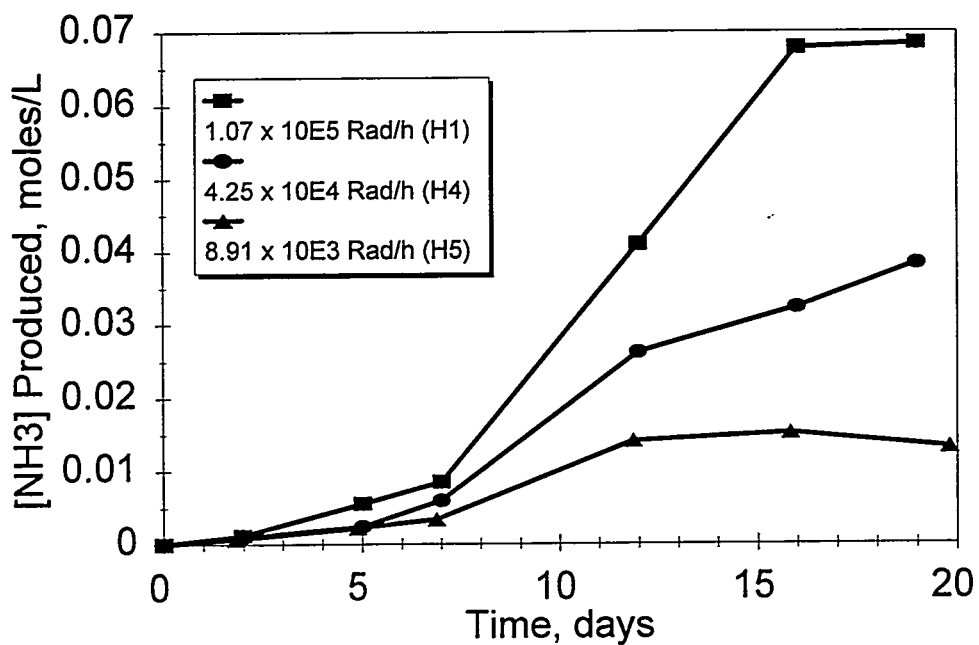


Figure 2.20. Gamma Dose Rate Dependence of Ammonia Production as a Function of Time in the Hydrolysis of IF-1B (0.5 g) at 90°C

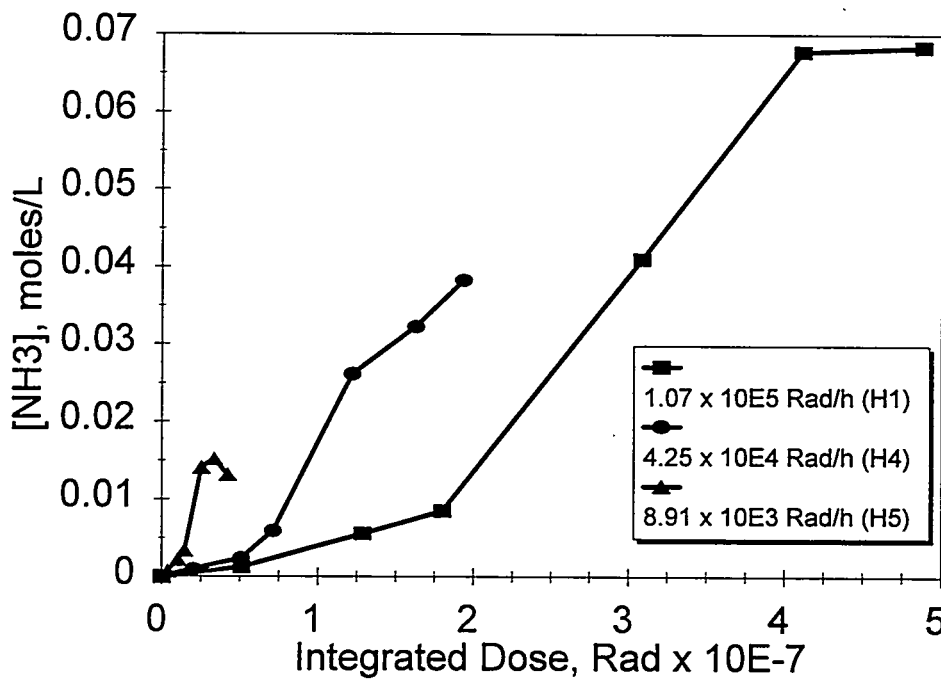


Figure 2.21. Ammonia Production as a Function of Integrated Dose (Rad x 10<sup>-7</sup>)

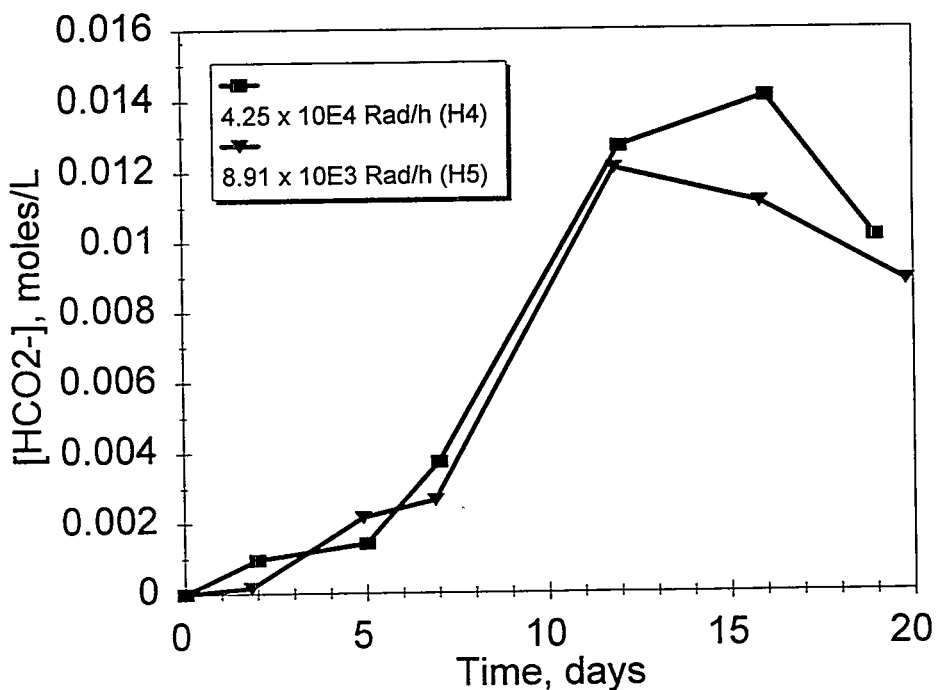


Figure 2.22. Formate Ion Production in the Hydrolysis of IF-1B in 2 M NaOH at 90°C and at Gamma Dose Rates of  $4.25 \times 10^4$  Rad/h (H4) and  $8.91 \times 10^3$  Rad/h (H5)

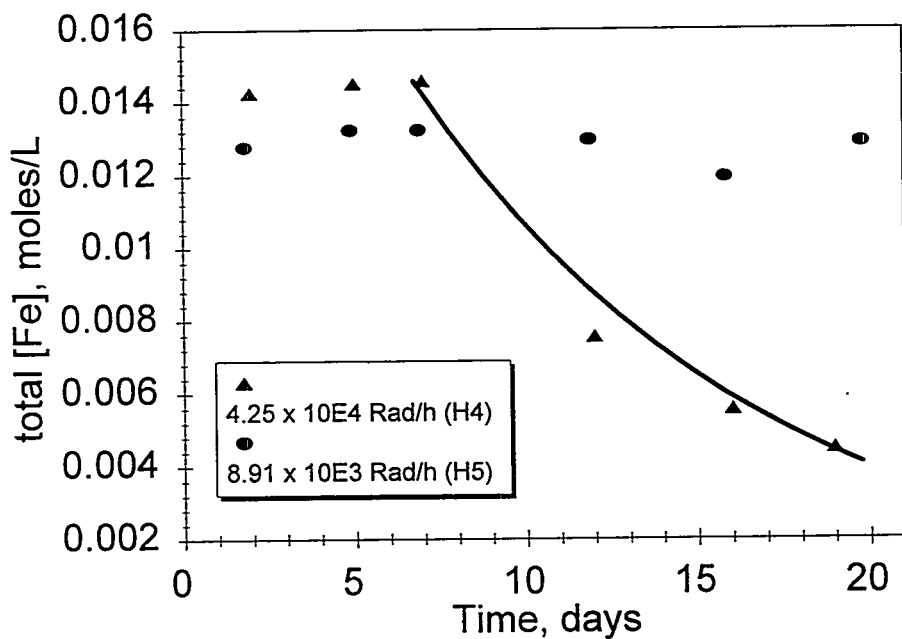
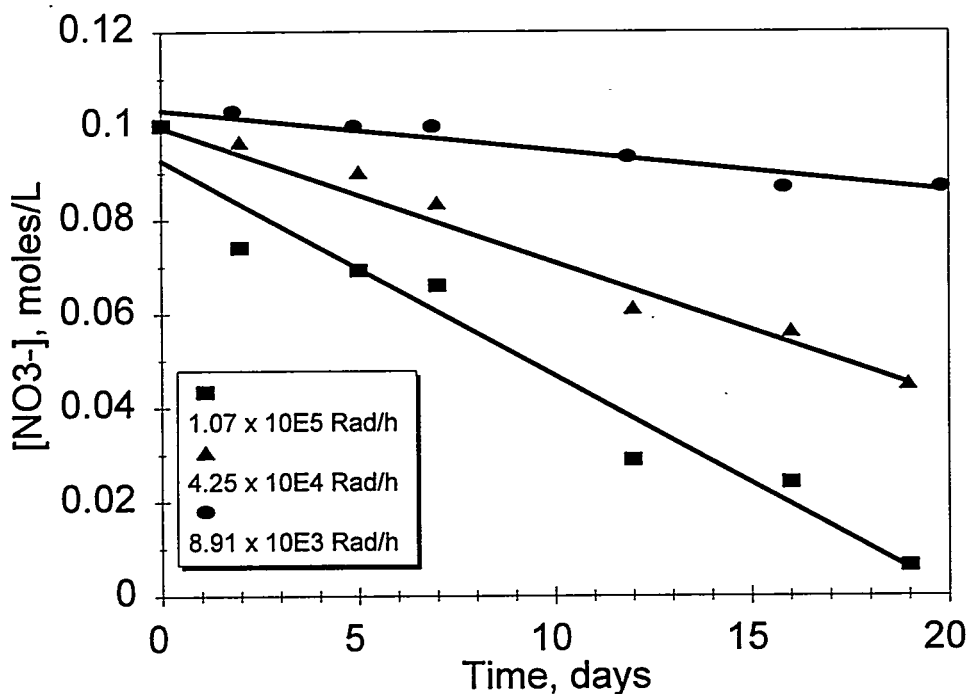


Figure 2.23. Total Iron Concentration as a Function of Time in the Hydrolysis of IF-1B (0.5 g) at 90°C and at Gamma Dose Rates of  $4.25 \times 10^4$  Rad/h (H4) and  $8.91 \times 10^3$  Rad/h (H5). Curved line represents calculated pseudo-first-order decrease in [Fe] for H4.

other soluble iron cyanides are formed until enough cyanide is destroyed that precipitation of insoluble iron species becomes favorable. Not enough data are available to specifically define when the drop in iron concentration in Experiment H4 starts, but, if the last four data points are assumed to represent a pseudo-first-order decrease in  $[Fe]$ , a rate constant of  $0.10 \text{ day}^{-1}$  is obtained. This constant is similar to that calculated from the H1 data ( $0.17 \text{ day}^{-1}$ ).

As in temperature dependence experiments, nitrate ion concentrations decreased and nitrite ion concentrations increased during the course of the hydrolysis experiments in the gamma field. The sum of these concentrations was about constant for each series of experiments. Zero-order plots of concentration versus time are linear as shown in Figures 2.24 and 2.25. Linear regression of the data (lines drawn through the data points) gives the rate constants shown in Table 2.7, and it is again seen that the rate of nitrate destruction equals the rate of nitrite formation. Table 2.7 also shows the general trend of increasing rate constant with increasing dose rate, but Figure 2.26 shows that the relationship is not linear.



**Figure 2.24.** Gamma Dose Rate Dependence of Nitrate Destruction in the Hydrolysis of IF-1B (0.5 g) at 90°C. Measured concentrations (data points) and zero-order fit (lines) are shown.

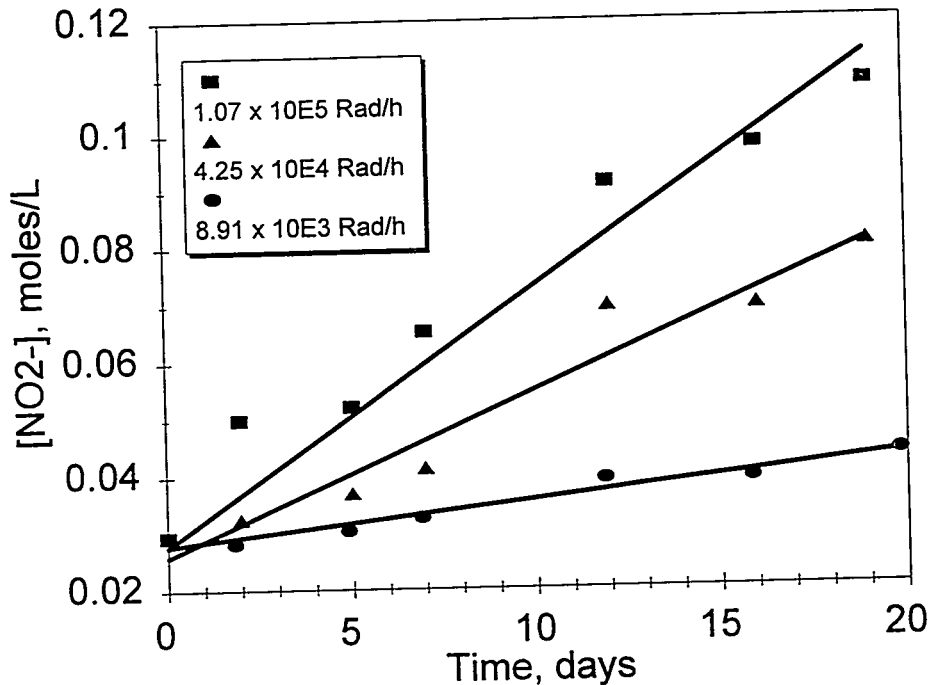


Figure 2.25. Gamma Dose Rate Dependence of Nitrite Formation in the Hydrolysis of IF-1B (0.5 g) at 90°C. Measured concentrations (data points) and zero-order fit (lines) are shown.

Table 2.7. Rate Constants for Nitrate Destruction and Nitrite Formation at Various Gamma Dose Rates

Experiment Number	Gamma Dose Rate (Rad/h)	NO <sub>2</sub> <sup>-</sup> Formation Rate Constant (moles/L/day)	NO <sub>3</sub> <sup>-</sup> Destruction Rate Constant (moles/L/day)
H1	1.07 x 10 <sup>5</sup>	4.5 x 10 <sup>-3</sup>	4.6 x 10 <sup>-3</sup>
H4	4.25 x 10 <sup>4</sup>	2.9 x 10 <sup>-3</sup>	2.9 x 10 <sup>-3</sup>
H5	8.91 x 10 <sup>3</sup>	7.8 x 10 <sup>-4</sup>	8.6 x 10 <sup>-4</sup>

### 2.3.3 Dependence of Hydrolysis on Ferrocyanide Ion Concentration

Experiments were conducted at half (H6) and twice (H7) the usual initial ferrocyanide ion concentration of 0.0127 M, which is obtained when 0.5 g IF-1B dissolves in 2 M NaOH. Table 2.8 summarizes the conditions used in these experiments. Recall that the portion of the ferrocyanide associated with cesium remains insoluble in this reaction medium (see Table 2.1).

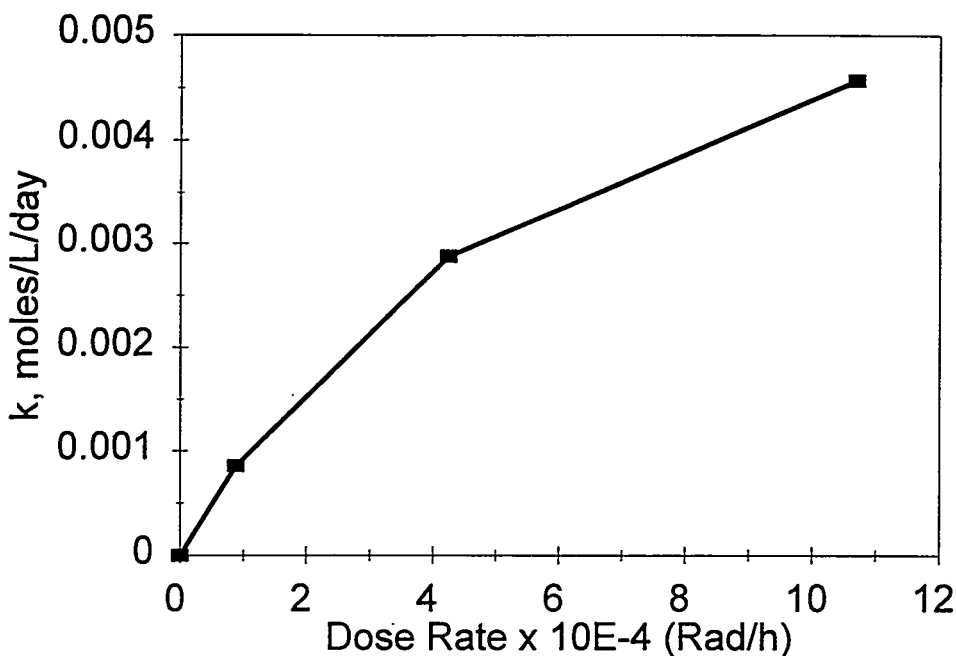
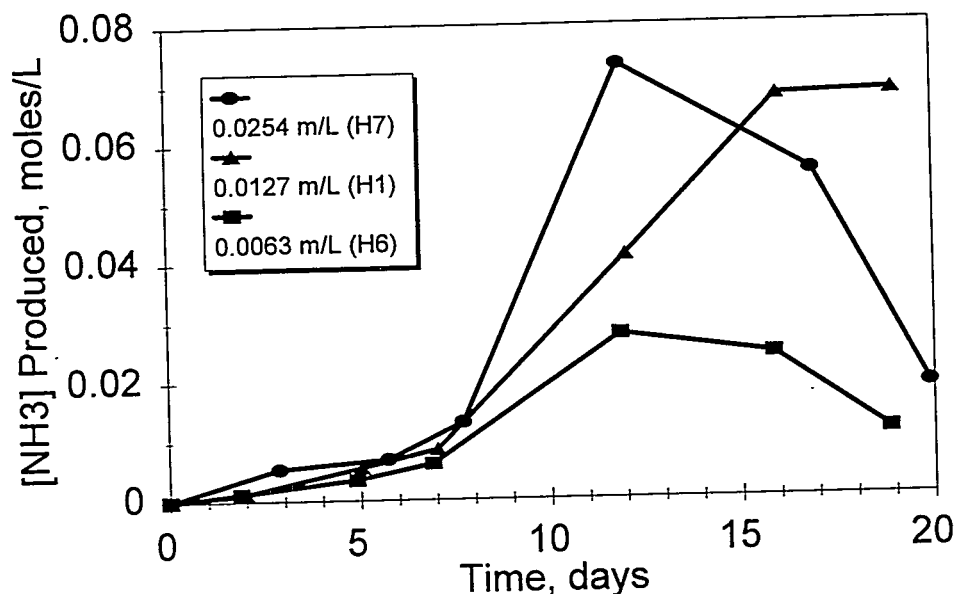


Figure 2.26. Rate Constants for Nitrate Ion Destruction as a Function of Gamma Dose Rate

Table 2.8. Conditions for IF-1B Hydrolysis Experiments Investigating the Effect of Ferrocyanide Ion Concentration Variation. Experiments conducted in 25 mL of 2 M NaOH for 3 weeks.

Experiment Number	Gamma Dose Rate (Rad/h)	Weight IF-1B (g)	Calc'd. $[\text{Fe}(\text{CN})_6^{-4}]$ (moles/L)	Temperature ( $^{\circ}\text{C}$ )
H6	$1.07 \times 10^5$	0.25	0.0063	90
H1	$1.07 \times 10^5$	0.5	0.0127	90
H7	$1.07 \times 10^5$	1.0	0.0254	90

Figure 2.27 illustrates the complexity of the reaction mechanism. The ammonia production behavior at half the usual concentration was normal, with a 7-day induction period, a period of more rapid  $\text{NH}_3$  production, and a period of decreased  $\text{NH}_3$  production. The maximum ammonia concentration accounted for about 70% of the theoretical maximum. The experiment at double the concentration (H7), however, showed much different behavior from that previously observed. After the induction period and rapid concentration increase, the ammonia concentration then rapidly decreased. The decrease in concentration occurred at a rate about five times that determined in the ammonia



**Figure 2.27.** Dependence of Ammonia Production on Initial Ferrocyanide Ion Concentration in Hydrolysis of IF-1B at 90°C and at a Gamma Dose Rate of  $1.07 \times 10^5$  Rad/h

irradiation control experiments discussed above. The formate ion concentration also rapidly decreased after Day 12 in Experiment H7 (Figure 2.28).

The change in soluble iron for H7 is also unusual (Figure 2.29). The concentration does not change from that expected for the initial solution until about Day 5, when the concentration drops off. Assuming pseudo-first-order behavior, the rate constant for the decrease in  $[\text{Fe}]$  is about  $0.12 \text{ day}^{-1}$ . This behavior is similar to that seen in Experiments H1 and H4. In contrast, an increase in  $[\text{Fe}]$  is seen on Day 19. It is unknown whether this increase in  $[\text{Fe}]$  corresponds to the sudden decrease in  $[\text{NH}_3]$ ; coordination of ammonia to iron would decrease the measured ammonia concentration. However, ferrous ammine complexes are reported to be stable only in concentrated ammonia solutions, and ferric ammine complexes are not stable (Klocke and Hixson 1972). Mixed iron cyanide/ammine complexes are known, but their stability in aqueous base is expected to be low (James et al. 1974).

Figures 2.30 and 2.31 show the zero-order decrease in nitrate concentration and increase in nitrite concentration. Table 2.9 shows that the rate constant for nitrate destruction is about equal to the rate of nitrite formation for each concentration investigated, as seen before. In addition, the destruction and formation processes show very little, if any, dependence on concentration.

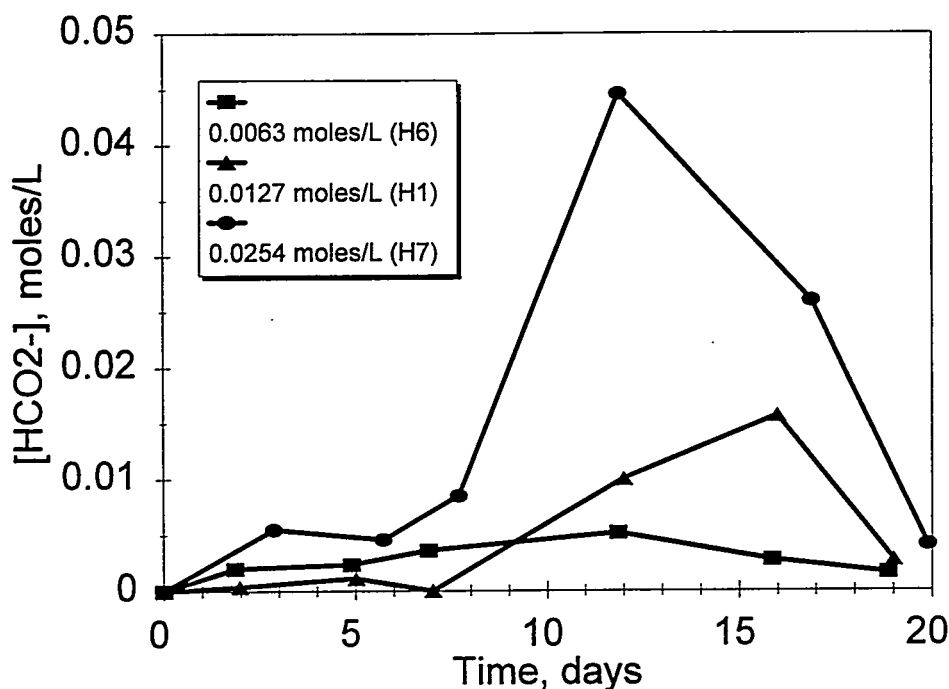


**Figure 2.28.** Dependence of Formate Ion Production on Initial Ferrocyanide Ion Concentration in Hydrolysis of IF-1B at 90°C and at a Gamma Dose Rate of  $1.07 \times 10^5$  Rad/h

## 2.4 Hydrolysis of In-Farm Ferrocyanide Flowsheet Material at pH 10

Cesium scavenging was performed at a pH in the range of 8 to 10. If waste added subsequently did not mix thoroughly, areas within the ferrocyanide waste might never have been exposed to high pH and may not have been heated to a high temperature. To investigate the behavior of such waste, IF-1B (0.5 g) was contacted with a pH 10 carbonate buffer (25 mL) containing 0.77 M NaNO<sub>3</sub> (to give a 1 M [Na<sup>+</sup>] solution), gamma-irradiated at  $1.07 \times 10^5$  Rad/h, and heated to 60°C for 3 months. Because of time and space considerations, only one irradiated sample and an identical non-irradiated control were prepared.

In the 3-month hydrolysis experiment, the irradiated solution contained  $2.96 \times 10^{-3}$  M NH<sub>3</sub>, while the non-irradiated control contained  $3.08 \times 10^{-4}$  M NH<sub>3</sub>, an order of magnitude less. Because ammonia is destroyed in the gamma field, the extent of hydrolysis will not be known until further analyses can be conducted. If no NH<sub>3</sub> destruction occurred, this yield would correspond to about 4 mole% ferrocyanide hydrolysis. However, with ammonia being destroyed at a zero-order rate of  $1.3 \times 10^{-3}$  m/L/day at this dose rate, a larger fraction of ferrocyanide was hydrolyzed after 3 months. The small degree of hydrolysis compared with that in 2 M NaOH was most likely due to the low solubility

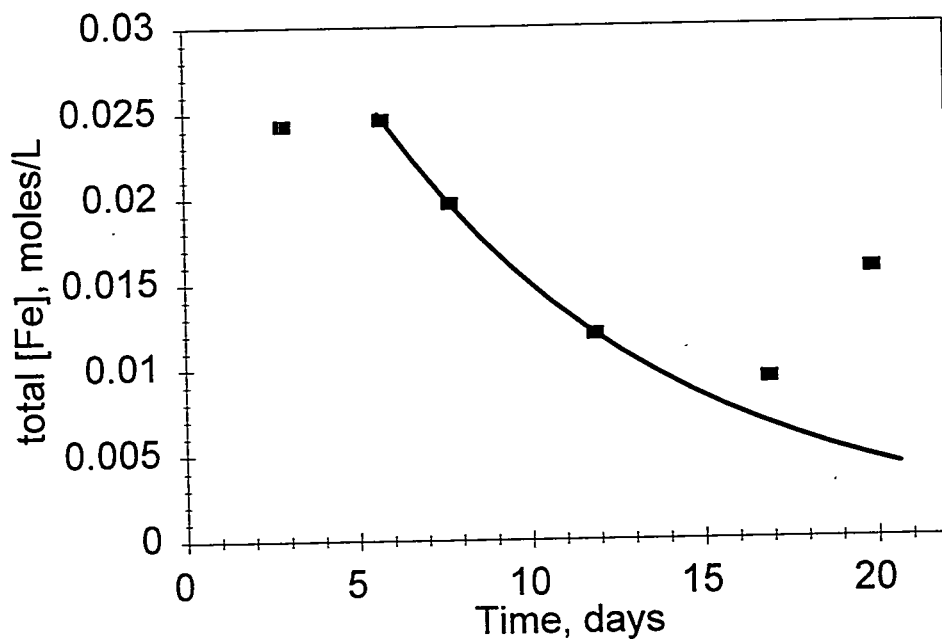


Figure 2.29. Total Iron Concentration as a Function of Time in Hydrolysis of IF-1B [ $0.0254\text{ M Fe(CN)}_6^{4-}$ ] at  $90^\circ\text{C}$  and at a Gamma Dose Rate of  $1.07 \times 10^5\text{ Rad/h}$  (H7)

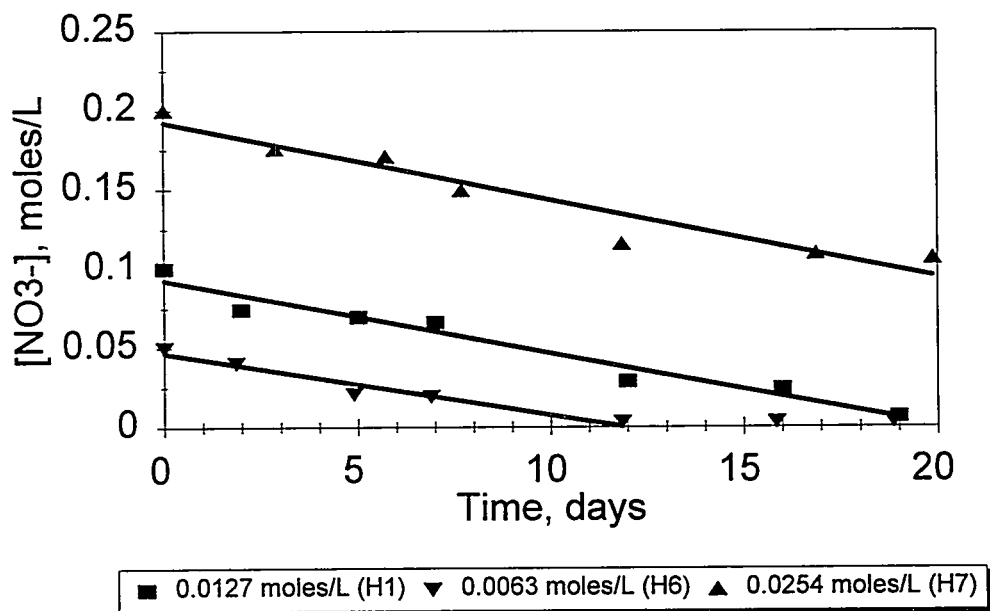
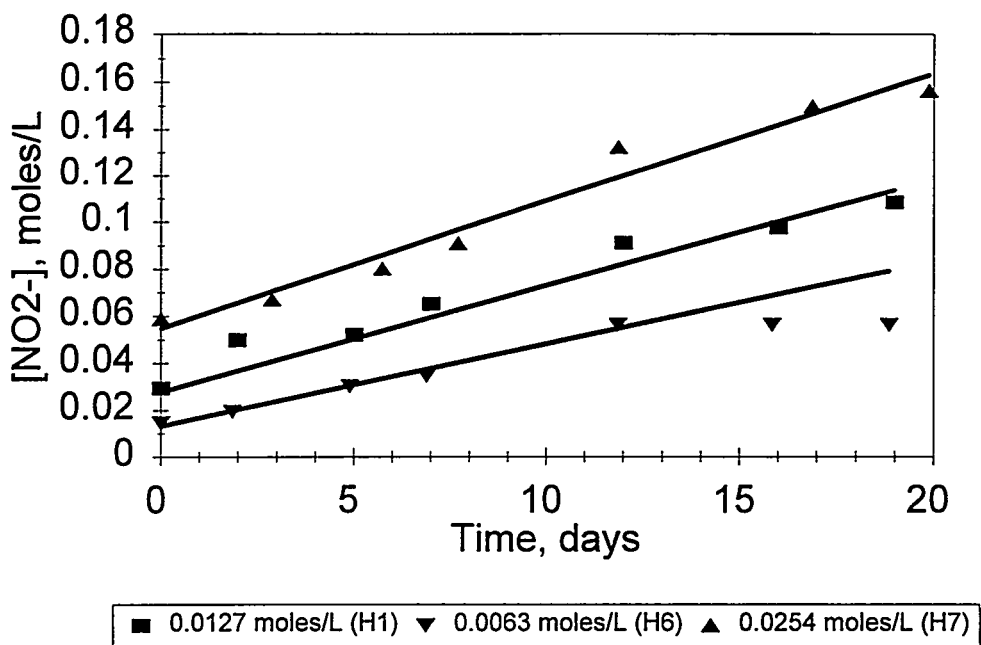


Figure 2.30. Ferrocyanide Ion Concentration Dependence of Nitrate Destruction in the Hydrolysis of IF-1B at  $90^\circ\text{C}$  and at a Gamma Dose Rate of  $1.07 \times 10^5\text{ Rad/h}$ . Measured concentrations (data points) and zero-order fit (lines) are shown.



**Figure 2.31.** Ferrocyanide Ion Concentration Dependence of Nitrite Formation in the Hydrolysis of IF-1B at 90°C and at a Gamma Dose Rate of  $1.07 \times 10^5$  Rad/h. Measured concentrations (data points) and zero-order fit (lines) are shown.

**Table 2.9.** Rate Constants for Nitrate Destruction and Nitrite Formation at Various Gamma Dose Rates

Experiment Number	Calc'd. Initial [NO <sub>2</sub> <sup>-</sup> ] (moles/L)	Calc'd. Initial [NO <sub>3</sub> <sup>-</sup> ] (moles/L)	NO <sub>2</sub> <sup>-</sup> Formation Rate Constant (moles/L/day)	NO <sub>3</sub> <sup>-</sup> Destruction Rate Constant (moles/L/day)
H6	0.015	0.050	$3.5 \times 10^{-3}$	$3.9 \times 10^{-3}$
H1	0.030	0.100	$4.5 \times 10^{-3}$	$4.6 \times 10^{-3}$
H7	0.060	0.200	$5.4 \times 10^{-3}$	$4.9 \times 10^{-3}$

of  $\text{Na}_2\text{NiFe}(\text{CN})_6$  at pH 10. The low solubility is reflected by the soluble iron concentration of  $1 \times 10^{-4} \text{ M}$  (0.7%), measured in the gamma irradiated solution at the conclusion of the experiment. The iron concentration in the control was at least one order of magnitude lower.

In a similar experiment conducted in FY 1993, very little hydrolysis of IF-1A was observed after 1 month of reaction at 60°C at a dose rate of  $1.43 \times 10^5$  Rad/h. The yield of ammonia in the irradiated

solution was 0.8% (not accounting for NH<sub>3</sub> destruction), and the amount of iron in solution corresponded to 0.2% dissolution. The control solution contained NH<sub>3</sub> corresponding to only 0.1% yield and essentially no soluble iron.

## 2.5 Hydrolysis of In-Farm Ferrocyanide Flowsheet Material in the Presence of an Aluminum Decladding Waste Simulant

Much of the waste added to the ferrocyanide precipitates in the tanks was aluminum decladding waste. A typical composition for neutralized aluminum coating waste generated by the bismuth phosphate process is shown in Table 2.10. A similar waste stream generated in PUREX processing was also added to tanks containing ferrocyanide waste.

The effect of aluminum on the hydrolysis reaction was investigated by preparing a simulant, the composition of which is also shown in Table 2.10, and contacting it with IF-1B. The simulant is similar to one bismuth phosphate process stream; however, concentrations in the tanks would be different depending on the compositions of other waste streams added, and on the composition of tank contents at the time of addition. Actual aluminum concentrations were probably less than that used in this experiment. Simulant solution (25 mL) was added to IF-1B (0.5 g), heated to 90°C, and irradiated at  $1.07 \times 10^5$  Rad/h for 3 weeks. Five irradiated and two control solutions were prepared and sampled with time.

Figure 2.32 shows the ammonia production for this experiment in comparison with Experiment H1, run under identical conditions except the hydrolysis solution was 2 M NaOH and did not contain aluminum. The initial stages of reaction appear identical until about Day 11 when ammonia production in the decladding waste simulant experiment apparently levels off. However, in a separate experiment, aluminum was found to interfere with the ammonia analysis.

**Table 2.10.** Neutralized Aluminum Coating Waste Composition Estimated from the Bismuth Phosphate Process and Composition of the Simulant Used for Hydrolysis Experiment H9

Component	Bismuth Phosphate Process Estimated Composition (mole/L)	Composition of Simulant Solution (mole/L)
NaAlO <sub>2</sub>	1.6	1.6
NaOH	1.5	1.5
NaNO <sub>3</sub>	0.9	0.9
NaNO <sub>2</sub>	1.2	1.2
Na <sub>2</sub> SiO <sub>3</sub>	0.01	0

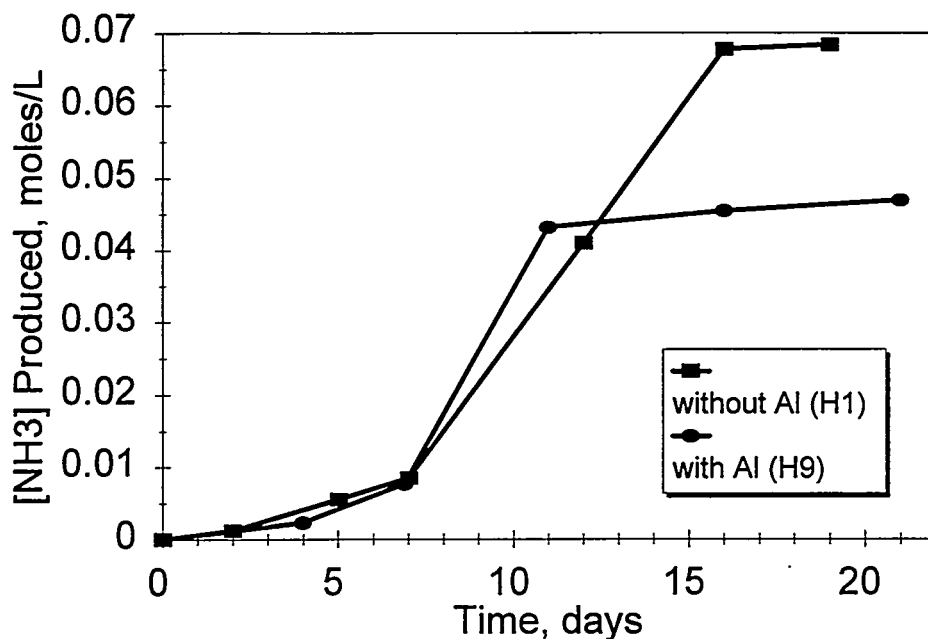


**Figure 2.32.** Ammonia Production in Hydrolysis of IF-1B (0.5 g) at 90°C and at a Gamma Dose Rate of  $1.07 \times 10^5$  Rad/h in the Absence (H1) and in the Presence (H9) of Aluminum

To test the ISE ammonia determination in the presence of aluminum, ammonium chloride (0.1 M aqueous solution) was added to basic stock solutions, similar to the neutralized aluminum coating waste simulant used in Experiment H9, to generate five solutions containing ammonia concentrations ranging from 0.2 to 0.8 M. The resulting diluted stock solutions also contained aluminum, nitrate, and nitrite, each at concentrations about five times less than in the analogous diluted H9 solutions that were analyzed for ammonia. Results of the ISE determination of ammonia in these five solutions (plus a blank not containing ammonia) are shown in Figure 2.33. The measured  $[\text{NH}_3]$  was found to be lower than the known concentration by up to 33%, the suppression in electrode reading increasing with increasing  $[\text{NH}_3]$ . The electrode response is seen to saturate at an observed  $[\text{NH}_3]$  of about 0.05 M. This behavior is very similar to what was observed in Experiment H9; the measured  $[\text{NH}_3]$  plateaus at about 0.045 M. Thus, it appears that the leveling-off in ammonia produced in Experiment H9 is an analytical artifact and not a suppression in hydrolysis activity by aluminum.

This conclusion is supported by the formate concentration data, shown in Figure 2.34. Formate is seen to continue to increase until Day 16, when the concentration decreases rapidly. The continued increase after Day 11, when the measured ammonia concentration plateaus, indicates that hydrolysis is continuing. The rapid decrease in formate concentration shows that the rate of formate destruction must be greater than the rate of its formation, suggesting that the hydrolysis reaction may be near completion. The same type of behavior is also seen (Figure 2.34) when aluminum is not present

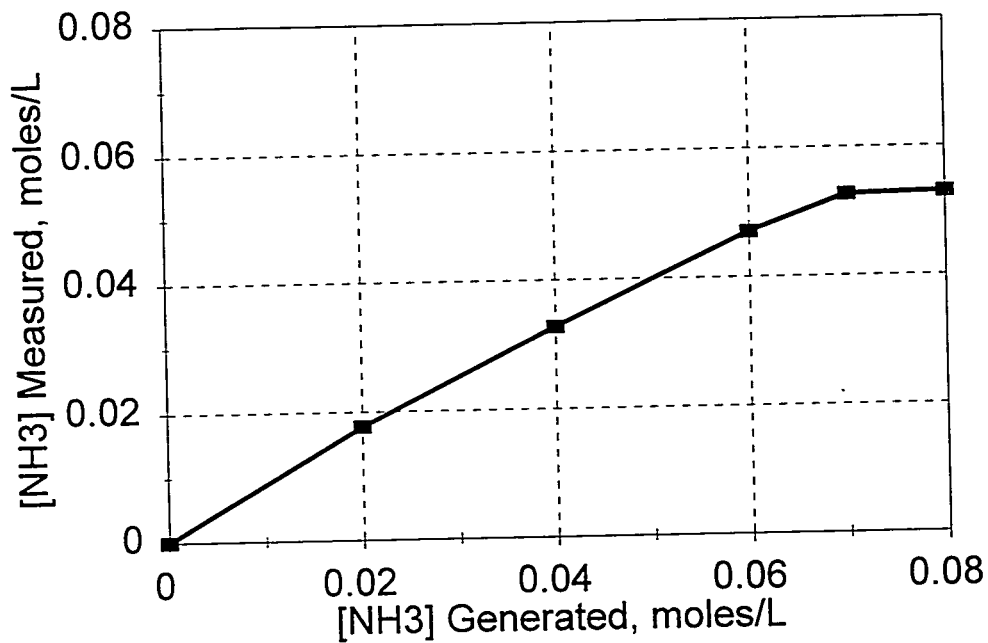


Figure 2.33. Measured Versus Known Ammonia Concentrations in Standard Solutions Containing Aluminum

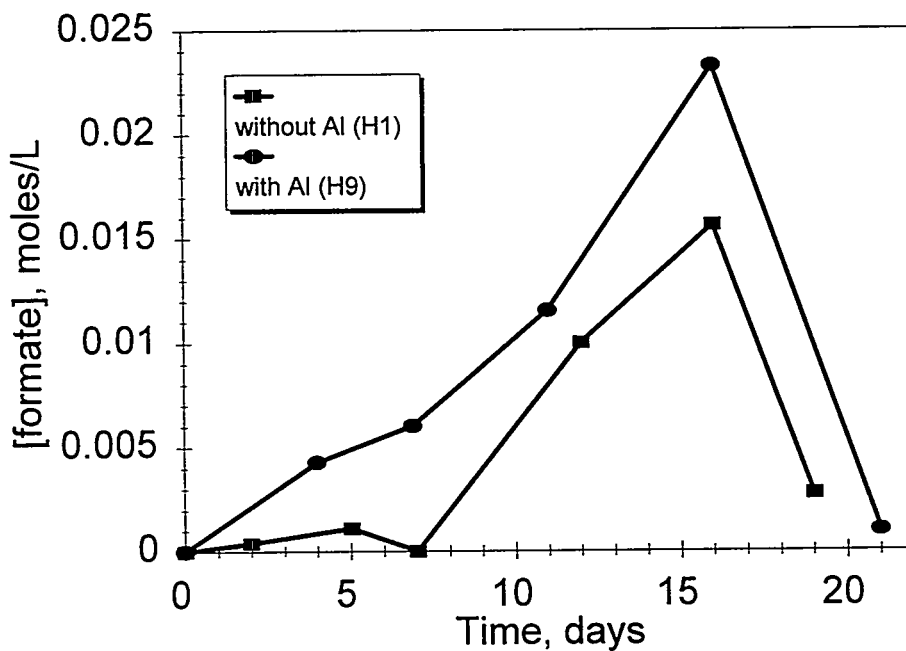
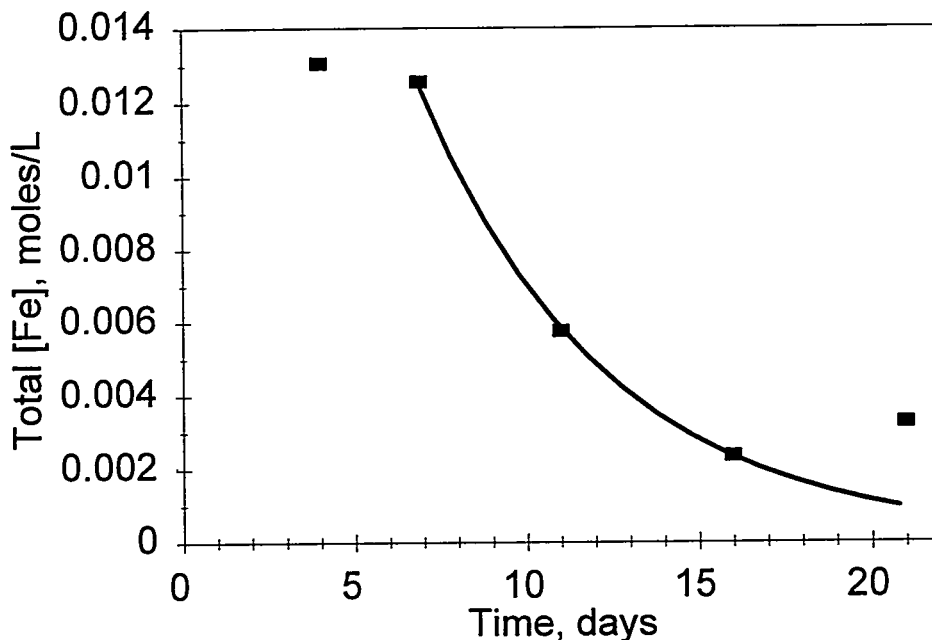


Figure 2.34. Formate Ion Production in Hydrolysis of IF-1B (0.5 g) at 90°C and at a Gamma Dose Rate of  $1.07 \times 10^5$  Rad/h in the Absence (H1) and in the Presence (H9) of Aluminum

(Experiment H1). In fact, the formate concentration data indicate that aluminum may enhance hydrolysis since formate ion is seen to increase more rapidly and reach a higher concentration in the presence of aluminum.

The change in total dissolved iron with time is shown in Figure 2.35 (data points). Like several previous experiments, the iron concentration remained about constant for nearly 7 days, at which time the concentration decreased in a pseudo-first-order way (line). The rate constant for this decrease was calculated to be  $0.18 \text{ day}^{-1}$ , very similar to the analogous experiment H1, in which the rate constant was calculated to be  $0.17 \text{ day}^{-1}$ . Unlike Experiment H1 and similar to Experiment H7, conducted at higher ferrocyanide ion concentration, an increase in soluble iron is observed at the conclusion of the experiment. The reason for this increase is unknown.



**Figure 2.35.** Total Iron Concentration as a Function of Time in Hydrolysis of IF-1B (0.5 g) at  $90^{\circ}\text{C}$  and at a Gamma Dose Rate of  $1.07 \times 10^5 \text{ Rad/h}$  in the Presence of Aluminum (H9). Curved line represents calculated pseudo-first-order decrease in [Fe].

### 3.0 Conclusions

The hydrolysis of ferrocyanide anion from In-Farm-1B, Rev. 7, an In-Farm flowsheet simulant, dissolved in 2 M NaOH has been investigated. The effects of gamma radiation ( $1.07 \times 10^5$ ,  $4.25 \times 10^4$ , and  $8.91 \times 10^3$  Rad/h), temperature (50°C, 70°C, and 90°C), and ferrocyanide anion concentration (0.0063, 0.0127, and 0.0254 M) were determined. Reactions were monitored as a function of time using analyses of dissolved  $[\text{NH}_3]$ ,  $[\text{Fe}]$ ,  $[\text{Ni}]$ ,  $[\text{Cs}]$ ,  $[\text{CN}^-]$ ,  $[\text{NO}_3^-]$ ,  $[\text{NO}_2^-]$ , and  $[\text{HCO}_2^-]$ .

Gamma radiation promotes the destruction of ferrocyanide anion by hydrolysis to ammonia. Yields of ammonia were found to be higher in reaction solutions exposed to gamma radiation than in identical solutions that were not irradiated. As the gamma dose rate increases, the rate of hydrolysis increases likewise. Similarly, increasing temperature and ferrocyanide anion concentration increases the rate of ammonia production. In 2 M NaOH, ferrocyanide destruction (by hydrolysis) of up to at least 90% has been observed, based on measured ammonia concentrations in solution. In general, ammonia production with time is sigmoidal. A 7-day induction period with slow ammonia production prior to a period of more rapid ammonia production suggests a complex reaction mechanism involving one or more intermediates. The total concentration of all soluble iron species, which often remains constant for several days followed by a pseudo-first-order decrease, also suggests the formation of iron-cyanide intermediates. The calculated rate constant for this decrease in  $[\text{Fe}]$  ranges from  $0.10 \text{ day}^{-1}$  to  $0.18 \text{ day}^{-1}$ . The solution ammonia concentration tends to level-off or decrease after 12 to 16 days. Decreasing concentration is a result of slow destruction in the gamma field. The leveling-off indicates that the rate of ammonia production is about the same as the rate of destruction, but does not necessarily indicate the approach to complete ferrocyanide anion destruction.

Cesium was not liberated in the hydrolysis experiments and presumably remains associated with ferrocyanide in the form of insoluble cesium-containing nickel ferrocyanide compounds. Nickel initially precipitates as  $\text{Ni}(\text{OH})_2$  when the flowsheet simulant reacts with aqueous base. However, free cyanide ion, liberated when ferrocyanide is destroyed, redissolves nickel as a nickel cyanide complex. The extent of redissolution depends on the free cyanide ion concentration. Nitrate ion is converted to nitrite ion in the gamma field at rates that are dependent on temperature and gamma dose rate, but independent of the initial nitrate ion concentration.

Hydrolysis occurs slowly at 60°C in a pH 10 solution. In the gamma field, an ammonia yield of at least 4 mole% was obtained. The relatively low yield is a result of the low solubility of  $\text{Na}_2\text{NiFe}(\text{CN})_6$  at this pH.

Aluminum does not inhibit, and may slightly promote, ferrocyanide hydrolysis. The presence of aluminum was found to interfere with the ammonia analysis method.

In competition experiments, cesium uptake by a ferrocyanide simulant not initially containing cesium was found to be more rapid than dissolution. Assuming that caustic waste added to the SSTs

contacted the ferrocyanide solids, these results suggest that cesium in the waste probably was immobilized in an insoluble ferrocyanide phase, even though much of the ferrocyanide was likely dissolved by such additions.

Continuing studies will provide more information about aging pathways and the kinetics of ferrocyanide hydrolysis. Further work is planned on the temperature and pH dependence of hydrolysis. The influence of waste tank components on aging will be addressed, and a study of the energy content of aged materials is planned.

## 4.0 References

- Anderson, J. D. 1990. *A History of the 200 Area Tank Farms*. WHC-MR-0132, Westinghouse Hanford Company, Richland, Washington.
- Borsheim, G. L., and B. C. Simpson. 1991. *An Assessment of the Inventories of the Ferrocyanide Watchlist Tanks*. WHC-SD-WM-ER-133 Rev. 0, Westinghouse Hanford Company, Richland, Washington.
- Bryan, S. A., K. H. Pool, S. L. Bryan, R. L. Sell, and L.M.P. Thomas. 1993. *Ferrocyanide Safety Program. Cyanide Speciation Studies FY 1993 Annual Report*. PNL-8887, Pacific Northwest Laboratory, Richland, Washington.
- Burger, L. L. 1984. *Complexant Stability Investigation, Task 1 - Ferrocyanide Solids*. PNL-5441, Pacific Northwest Laboratory, Richland, Washington.
- Burger, L. L., and R. D. Scheele. 1988. *Interim Report - Cyanide Safety Studies*. PNL-7175, Pacific Northwest Laboratory, Richland, Washington.
- Burger, L. L., and R. D. Scheele. 1991. *The Reactivity of Cesium Nickel Ferrocyanide Towards Nitrate and Nitrite Salts - A Status Report*. PNL-7550, Pacific Northwest Laboratory, Richland, Washington.
- Burger, L. L., D. A. Reynolds, W. W. Schulz, and D. M. Strachan. 1991. *A Summary of Available Information on Ferrocyanide Tank Wastes*. PNL-7822, Pacific Northwest Laboratory, Richland, Washington.
- Butler, J. N. 1964. *Ionic Equilibrium, a Mathematical Approach*. Addison-Wesley Publishing Company, Inc., Reading, Massachusetts.
- Cady, H. H. 1993. *Evaluation of Ferrocyanide/Nitrate Explosive Hazard*. LA-12589-MS, Pacific Northwest Laboratory, Richland, Washington.
- Campbell, D. O., D. D. Lee, and T. A. Dillow. 1990. "Low-Level Liquid Waste Decontamination by Ion Exchange." *Waste Management '90*, ed. R. G. Post. 2:389-398.
- Christensen, J. J., R. M. Izatt, J. D. Hale, R. T. Pack, and G. D. Watt. 1963. "Thermodynamics of Metal Cyanide Coordination. II.  $\Delta G^\circ$ ,  $\Delta H^\circ$ , and  $\Delta S^\circ$  Values for Tetracyanonickelate(II) Ion Formation in Aqueous Solution at 25°C." *Inorg. Chem.* 2:337-339.

- Crowe, R. D., M. Kummerer, and A. K. Postma. 1993. *Estimation of Heat Load in Waste Tanks Using Average Vapor Space Temperatures*. WHC-EP-0709, Westinghouse Hanford Company, Richland, Washington.
- Deaton, D. E. 1990. *Unusual Occurrence-Unreviewed Safety Questions Regarding Tanks Containing Ferrocyanide*. WHC-90-B003-R1, Update 10-22-90, Westinghouse Hanford Company, Richland, Washington.
- Dodds, J. N., and W. J. Thompson. 1994. "DXRD Studies of Sodium Nickel Ferrocyanide Reactions with Equimolar Nitrate/Nitrite Salts." *Environ. Sci. Technol.* 28(5):882-889.
- Edwards, T. J., G. Maurer, J. Newman, and J. M. Prausnitz. 1978. "Vapor-Liquid Equilibria in Multicomponent Aqueous Solutions of Volatile Weak Electrolytes." *American Institute of Chemical Eng. Journal* 24:966.
- Epstein, M., and H. K. Fauske. 1994. *Conditions for Reaction Propagation in Dried Ferrocyanide/Nitrate-Nitrite Powders*. WHC-SD-WM-TI-619, Rev. 0, Westinghouse Hanford Company, Richland, Washington.
- Goldstein, S., G. Czapski, H. Cohen, and D. Meyerstein. 1988. "Formation and Decomposition of Iron-Carbon  $\sigma$ -Bonds in the Reaction of Iron(III)-Poly(amino carboxylate) Complexes with  $\text{CO}_2^-$  Free Radicals. A Pulse Radiolysis Study." *J. Am. Chem. Soc.* 110(12):3903-3907.
- Hallen, R. T., L. L. Burger, R. L. Hockey, M. A. Lilga, R. D. Scheele, and J. M. Tingey. 1992. *Ferrocyanide Safety Project FY 1991 Annual Report*. PNL-8165, Pacific Northwest Laboratory, Richland, Washington.
- Hepworth, J. L., E. D. McClanahan, and R. L. Moore. 1957. *Cesium Packaging Studies - Conversion of Zinc Ferrocyanide to a Cesium Chloride Product*. HW-48832, Hanford Atomic Products Operation, Richland, Washington.
- James, A. D., R. S. Murray, and W.C.E. Higginson. 1974. "Iron(II) Catalysis in Substitution Reactions of Amminepentacyano- and Aquopentacyano-ferrate(III) Ions." *J. Chem. Soc., Dalton Trans.* 1273-1278.
- Jeppson, D. W., and J. J. Wong. 1993. *Ferrocyanide Waste Simulant Characterization*. WHC-EP-0631, Westinghouse Hanford Company, Richland, Washington.
- Klocke, D. J., and A. N. Hixson. 1972. "Solubility of Ferrous Iron in Aqueous Ammoniacal Solutions." *Ind. Eng. Chem. Process Des. Develop.* 11(1):141-146.

- Lilga, M. A., M. R. Lumetta, W. F. Riemath, R. A. Romine, and G. F. Schiefelbein. 1992. *Ferrocyanide Safety Project, Subtask 3.4, Aging Studies FY 1992 Annual Report*. PNL-8387, Pacific Northwest Laboratory, Richland, Washington.
- Lilga, M. A., M. R. Lumetta, and G. F. Schiefelbein. 1993. *Ferrocyanide Safety Project, Task 3 Ferrocyanide Aging Studies FY 1993 Annual Report*. PNL-8888, Pacific Northwest Laboratory, Richland, Washington.
- Loewenschuss, H. 1982. "Metal-Ferrocyanide Complexes for the Decontamination of Cesium from Aqueous Radioactive Waste." *Radioactive Waste Management* 2(4):327-341.
- Loos-Neskovic, C., and M. Fedoroff. 1989. "Fixation Mechanisms of Cesium on Nickel and Zinc Ferrocyanides." *Solvent Extraction and Ion Exchange* 7(1):131-158.
- Loos-Neskovic, C., M. Fedoroff, and G. Revel. 1976. "Influence of Sodium Content of Nickel Ferrocyanides on the Retention of Alkaline Ions." *Radiochem. Radioanal. Letters* 26(1):17-26.
- Loos-Neskovic, C., M. Fedoroff, and M. O. Mecherri. 1990. "Ion Fixation Kinetics and Column Performance of Nickel and Zinc Hexacyanoferrates(II)." *Analyst* 115:981-986.
- McGrail, B. P., D. S. Trent, G. Terrones, J. D. Hudson, and T. E. Michener. 1993. *Computational Analysis of Fluid Flow and Zonal Deposition in Ferrocyanide Single-Shell Tanks*. PNL-8876, Pacific Northwest Laboratory, Richland, Washington.
- McLaren, J. M. 1993. *Ferrocyanide Safety Program: Updated Thermal Analysis Model for Ferrocyanide Tanks with Application to Tank 241-BY-104*. WHC-EP-0669, Westinghouse Hanford Company, Richland, Washington.
- McLaren, J. M. 1994. *Ferrocyanide Safety Program: Thermal Analysis of Ferrocyanide Tanks, Group I*. WHC-EP-0729, Westinghouse Hanford Company, Richland, Washington.
- McLaren, J. M., and R. J. Cash. 1993. *Ferrocyanide Safety Program: Heat Load and Thermal Characteristics Determination for Selected Tanks*. WHC-EP-0638, Westinghouse Hanford Company, Richland, Washington.
- Meacham, J. E., R. J. Cash, and G. T. Dukelow. 1994. *Quarterly Report on the Ferrocyanide Safety Program for the Period Ending June 30, 1994*. WHC-EP-0474-13, Westinghouse Hanford Company, Richland, Washington.
- Norton, J. D., and L. R. Pederson. 1994. *Ammonia in Simulated Hanford Double-Shell Tank Wastes: Solubility and Effects on Surface Tension*. PNL-10173, Pacific Northwest Laboratory, Richland, Washington.

Parra, S. A. 1994. *Integrated Beta and Gamma Radiation Dose Calculations for the Ferrocyanide Waste Tanks*. WHC-SD-WM-TI-634, Rev. 0, Westinghouse Hanford Company, Richland, Washington.

Peach, J. D. 1990. "Consequences of Explosion of Hanford's Single-Shell Tanks Are Understated." Letter B-241479 dated October 1990 to M. Synar, GAO/RCED-91-34, General Accounting Office, Washington, D.C.

Postma, A. K., J. E. Meacham, G. S. Barney, G. L. Borsheim, R. J. Cash, M. D. Crippen, D. R. Dickinson, J. M. Grigsby, D. W. Jeppson, M. Kummerer, J. M. McLaren, C. S. Simmons, and B. C. Simpson. 1994. *Ferrocyanide Safety Program: Safety Criteria for Ferrocyanide Watch List Tanks*. WHC-EP-0691, Westinghouse Hanford Company, Richland, Washington.

Robuck, S. J., and R. G. Luthy. 1989. "Destruction of Iron-Complexed Cyanide by Alkaline Hydrolysis." *Wat. Sci. Tech.* 21:547-558.

Rocklin, R. D., and E. L. Johnson. 1983. "Determination of Cyanide, Sulfide, Iodide, and Bromide by Ion Chromatography with Electrochemical Detection." *Anal. Chem.* 55:4-7.

Scheele, R. D., and H. H. Cady. 1992. *Preliminary Safe-Handling Experiments on a Mixture of Cesium Nickel Ferrocyanide and Equimolar Sodium Nitrate/Nitrite*. PNL-7928, Pacific Northwest Laboratory, Richland, Washington.

Scheele, R. D., L. L. Burger, J. M. Tingey, S. A. Bryan, G. L. Borsheim, B. C. Simpson, R. J. Cash, and H. H. Cady. 1991. "Ferrocyanide-Containing Waste Tanks: Ferrocyanide Chemistry and Reactivity." PNL-SA-19924, presented at *Environmental Restoration 1991*, University of Arizona, Tucson, Arizona.

Scheele, R. D., L. L. Burger, J. M. Tingey, R. T. Hallen, and M. A. Lilga. 1992. "Chemical Reactivity of Potential Ferrocyanide Precipitates in Hanford Tanks with Nitrates and Nitrites." In *Proceedings of Waste Management '92*, Tucson, Arizona.

U.S. Department of Energy (DOE). 1987. *Final Environmental Impact Statement, Disposal of Hanford Defense High-Level, Transuranic, and Tank Wastes*. DOE-EIS-0113, Washington, D.C.

## Distribution

No. of  
Copies

No. of  
Copies

### OFFSITE

12 U.S. Department of Energy  
Office of Scientific and  
Technical Information

Charles S. Abrams  
1987 Virginia  
Idaho Falls, ID 83404

Shirley Campbell-Grizzel  
U.S. Department of Energy  
EH-15, Trevion II  
12800 Middlebrook Road  
Germantown, MD 20874

George E. Schmauch  
Air Products & Chemicals, Inc.  
7201 Hamilton Blvd.  
Allentown, PA 18195-1501

James A. Gieseke  
Battelle Columbus Division  
505 King Avenue  
Columbus, OH 43201-2693

Kamal K. Bandyopadhyay  
Brookhaven National Laboratory  
Upton, NY 11973

David O. Campbell  
102 Windham Road  
Oak Ridge, TN 37830

Fred N. Carlson  
6965 North 5th West  
Idaho Falls, ID 83401

Gary Powers  
Design Science, Inc.  
163 Witherow Road  
Sewickley, PA 15143

Hans K. Fauske  
Fauske and Associates, Inc.  
16W070 W. 83rd St.  
Burr Ridge, IL 60521

Gregory R. Choppin  
Florida State University  
Department of Chemistry B-164  
Tallahassee, FL 32306

Melvin W. First  
Harvard University  
295 Upland Avenue  
Newton Highlands, MA 02161

Chester Grelecki  
Hazards Research Corporation  
200 Valley Road, Suite 301  
Mt. Arlington, NJ 07856

Billy Hudson  
202 Northridge Court  
Lindsborg, KA 67456

Thomas S. Kress  
P.O. Box 2009  
9108, MS-8088  
Oak Ridge, TN 37831-8088

No. of  
Copies

No. of  
Copies

3 Los Alamos National Laboratory  
P.O. Box 1663  
Los Alamos, NM 87545  
Steve F. Agnew  
Steve Eisenhower  
Thomas E. Larson

Mujid S. Kazimi  
MIT/Dept of Nuclear Eng.  
77 Massachusetts Avenue  
Room 24-102  
Cambridge, MA 02139

Louis Kovach  
Nuclear Consulting Services, Inc.  
P.O. Box 29151  
Columbus, OH 43229-0151

2 Oak Ridge National Laboratory  
P.O. Box 2008  
Oak Ridge, TN 37831-6385  
Emory D. Collins, MS-6385  
Charles W. Forsberg, MS-6495

Arlin K. Postma  
3640 Ballard Road  
Dallis, OR 97338

William R. Prindle  
1556 Crestline Drive  
Santa Barbara, CA 93105

Andrew S. Veletsos  
Rice University  
5211 Paisley  
Houston, TX 77096

2 Sandia National Laboratory  
P.O. Box 5800  
Albuquerque, NM 87185  
Scott E. Slezak, MS-0741  
Dana Powers, MS-0744

Alfred Schneider  
5005 Hidden Branches Drive  
Dunwoody, GA 30338

3 Ray S. Daniels  
Science Applications International  
Corporation  
20300 Century Blvd., Suite 200-B  
Germantown, MD 20874

Michael T. Gordon  
State of Washington  
Department of Ecology  
P. O. Box 47600  
Olympia, WA 98504-7600

Alex Stone  
1105 W. 10th Ave., #236  
Kennewick, WA 99336-6018

6 U.S. Department of Energy  
EM-36, Trevion II  
12800 Middlebrook Road  
Germantown, MD 20874  
James V. Antizzo  
Charles O'Dell (5)

Thomas C. Temple  
U.S. Department of Energy  
Savannah River Operations Office  
P.O. Box A  
Aiken, SC 29808

No. of  
Copies

No. of  
Copies

Bruce R. Kowalski  
University of Washington  
Center for Process Analytical  
Chemistry  
Chemistry Department BG-10  
Seattle, WA 98195

Joseph S. Byrd  
University of South Carolina  
Department of Electrical and  
Computer Engineering  
Swearingen Engineering Center  
Columbia, SC 29208

Frank L. Parker  
Vanderbilt University  
P.O. Box 1596, Station B  
Nashville, TN 37235

Donald T. Oakley  
Waste Policy Institute  
555 Quince Orchard Road,  
Ste 600  
Gaithersburg, MD 20878-1437

**FOREIGN**

Claude Musikas  
Consultant  
5, Avenue Moissan,  
91440 Bures/Yvette,  
France

**ONSITE**

**13 U.S. Department of Energy  
Richland Operations Office**

R. F. Christensen, S7-54 (4)  
R. E. Gerton, S7-54 (4)  
W. F. Hendrickson, S7-54  
A. G. Krasopoulos, A4-81  
Public Reading Room, H2-53  
RL Docket File, H5-36 (2)

**37 Westinghouse Hanford Company**

H. Babad, S7-30  
J. B. Billetdeaux, S7-16  
D. C. Board, S1-57  
G. L. Borsheim, H5-27  
R. J. Cash, S7-15 (2)  
M. D. Crippen, L5-31  
D. R. Dickinson, L5-31  
G. T. Dukelow, S7-15  
J. M. Grigsby, H4-62  
M. E. Huda, R3-08  
M. N. Islam, R3-08  
D. W. Jeppson, L5-31  
N. W. Kirch, R2-11  
C. A. Kuhlman, B3-30  
M. Kummerer, H4-62  
J. M. McLaren, H0-34  
J. E. Meacham, S7-15  
N. J. Milliken, H4-63  
S. R. Moreno, B3-06

No. of  
Copies

No. of  
Copies

M. A. Payne, S7-14  
F. R. Reich, L5-55  
C. P. Schroeder, L7-06  
B. C. Simpson, R2-12  
H. Toffer, H0-38  
W. T. Watson, H0-38  
W. D. Winkelman, L5-55  
D. D. Wodrich, S7-84  
W. F. Zuroff, S7-12  
Central Files, L8-04  
Document Processing and  
Distribution, L8-15 (2)  
EDMC, H6-08  
Information Release  
Administration, R1-05 (3)  
TFIC, R1-20

**44 Pacific Northwest Laboratory**

E. V. Alderson, P8-38  
E. G. Baker, P8-38  
R. M. Bean, P8-08

J. W. Brothers, K5-22  
S. A. Bryan, K5-82  
L. L. Eyler, K7-15  
L. L. Fassbender, K8-18  
A. R. Felmy, K6-82  
S. R. Gano, P8-38  
S. C. Goheen, P8-08  
B. M. Johnson, K1-78  
D. J. Kowalski, P8-38  
M. A. Lilga, P8-38 (15)  
G. J. Lumetta, P7-25  
M. R. Lumetta, P8-38  
B. P. McGrail, K2-38  
L. R. Pederson, K2-44  
A. W. Prichard, K8-34  
D. Rai, K6-82  
R. D. Scheele, P7-25  
G. F. Schiefelbein, P8-38 (2)  
C. W. Stewart, K7-15  
D. M. Strachan, K2-44  
Publishing Coordination  
Technical Report Files (5)